N. A. E.

R. & M. No. 2894
(11,602, 11,883)
A.R.C. Technical Report

MINISTRY OF SUPPLY

AERONAUTICAL RESEARCH COUNCIL
REPORTS AND MEMORANDA

A Wind-tunnel Investigation of Entry Loss on Propeller Turbine Installations

Parts I and II

By

J. SEDDON, Ph.D.
and
A. SPENCE, B.Sc.

LONDON: HER MAJESTY'S STATIONERY OFFICE
1954

PRICE 14*s* 6*d* NET

A Wind-tunnel Investigation of Entry Loss on Propeller Turbine Installations

Parts I and II

By

J. SEDDON, Ph.D.
and
A. SPENCE, B.Sc.

COMMUNICATED BY THE PRINCIPAL DIRECTOR OF SCIENTIFIC RESEARCH (AIR), MINISTRY OF SUPPLY

Reports and Memoranda No. 2894*
August, 1948

Summary.—The report is in two parts, following a general introduction. Part I describes wind-tunnel tests on

(*a*) a series of models of annular entries, with and without propeller, in the 5-ft tunnel;

(*b*) a set of large circular blade roots on a full-size nacelle in the 24-ft tunnel.

The models were based on two representative propeller turbine engines of different sizes. Various shapes and sizes of spinner and duct were tested, including 'vertical' and 'sloped' entries and 'elliptical' and 'conical' spinners. The work follows on from past tests, model and full-scale, on entries for radial air-cooled reciprocating engines.

The smaller engine tends to have the higher entry loss, owing to the blade roots being relatively thicker. In a typical case, under cruising conditions, the total entry loss on the model is 25 per cent of free-stream dynamic head, of which 15 per cent is caused by the blade roots. Scale effect is likely to be small. In these circumstances a large diameter spinner gives the best result. Sloped entries are not recommended.

From a generalised analysis of the results empirical rules are suggested for the estimation of spinner loss, duct loss, and blade-root loss, making up the total entry loss in flight. The additional duct loss which is usually present in ground running is also considered in general terms.

Part II describes wind-tunnel tests on models of a number of alternative ducted spinners for a typical engine, and, for comparison, one annular entry similar to those tested in Part I.

It is shown that the ducted spinners give 90 to 95 per cent total head in cruising flight compared with about 75 per cent for the annular entry. Most of the gain is in a reduction of blade root loss from 17 per cent total head to about 2 per cent. The results are not sensitive to the shape of the blade root fairing.

Low velocity must be maintained as far as possible, both in the spinner itself and in the rear duct. Expansion of the duct in the neighbourhood of the leak should be avoided, however. The leak gap should be kept small, to minimise the extra flow taken through the spinner.

A short cowl version, in which the outer cowl of the spinner terminates just ahead of the propeller, is satisfactory for practical purposes, and has the advantage of being lighter in weight than a long cowl spinner with nose entry.

A detailed analysis of the loss is given, using methods evolved in Part I.

*R.A.E. Report Aero 2252, received 26th June, 1948.

R.A.E. Report Aero 2281, received 3rd November, 1948.

A

General Introduction.—A series of wind-tunnel tests has been made to determine the loss of total head in various forms of air intake for propeller turbine engines with tractor propellers. There are two main parts to the investigation and these are described separately in the body of the report. Part I deals with the most usual arrangement, in which the air is taken in at an annular entry directly behind the rotating propeller and spinner. The tests and analyses lead to generalisations on blade-root blockage and on the additional loss present under ground running conditions. Part II describes a series of tests on ducted spinners and compares the results with those for annular intakes.

The work is confined to intakes for direct-flow engines with axial compressors. With a reverse-flow engine or a plenum chamber installation the ducted part of the intake would be different in form from those tested. The conclusions on propeller losses, however, can be applied to any form of annular intake.

PART I

Annular Entries Behind Propellers

1. *Introduction.*—1.1. *Component Losses, and Velocity Ratio.*—The annular intake in the nose of a nacelle or body, close behind the blade roots of a rotating propeller (Fig. 1a) is aerodynamically one of the more complicated types of air intake. The total entry loss consists of three more or less distinct parts. These are:

(*a*) the spinner loss, arising from boundary-layer development, and possibly separation, on the nose fairing or propeller ' spinner '

(*b*) the duct loss, from friction or expansion losses in the annular duct

(*c*) the blade-root loss, caused by the drag and interference of the propeller roots.

An important concept is the ' velocity ratio ', defined as the ratio of flight speed, V, to a representative velocity in the duct, usually the mean entry velocity V_i. Previously the term ' entry velocity ratio ' has been used to denote the inverse ratio V_i/V ; but recent work including the present, has shown the advantage of having the more nearly constant velocity (that in the duct) as denominator. The chief added convenience is that of being able to examine results for the whole flight range, including ground running ($V = 0$), in a single unified form. In the present analysis, the mean velocity V_c at the compressor (*i.e.*, at the end of the duct) is sometimes used in preference to V_i to define the velocity ratio. This is useful, for example, when making direct comparison between results for different intakes for the same engine, having identical conditions at the compressor, but different entry sizes and hence different values of V_i.

The velocity ratio at entry has an important effect on the relative proportions of the component losses, and on the magnitude of the total loss. Normally the first consideration in a design is to ensure low duct loss by making the duct area large, which implies a high velocity ratio for a given flight speed. But the higher the velocity ratio, the greater is the rise of pressure accompanying the retardation ahead of the entry, and this may react adversely on both the other loss components. In particular, for a given spinner, there will be a limiting value of the velocity ratio above which the flow over the spinner is unstable and local separations occur. By reducing the entry area, giving a lower velocity ratio at the same flight speed, a stable flow can be obtained, with a corresponding reduction in spinner loss ; but generally speaking this will increase the duct loss.

Fig. 2 shows a typical entry-loss curve for an annular entry without propeller. The loss of total head, expressed in terms of the mean entry dynamic head $\frac{1}{2}\rho V_i^2$, is plotted against velocity ratio V/V_i. The limiting velocity ratio is indicated, above which the loss increases rapidly

owing to the breakdown of flow over the spinner. At the other end of the range, in ground running, an additional loss usually occurs, caused by high velocities or flow separation just inside the entry lip. At moderate flight speeds, when the velocity ratio is near unity, the loss is a minimum.

1.2. *Past Work on Reciprocating Engines.*—We are familar with the annular entry on radial air-cooled reciprocating engines. Past work on these has been summarised in Ref. 1. Very few systematic data were obtained, but certain broad features of the results can now be seen. The total entry loss up to the cylinders, in level cruise, was generally of the order of $0{\cdot}3q$*. Flow separation occurred often on the spinners, but it was profitable nevertheless to maintain a high velocity ratio, because with smaller entries the duct loss became excessive. The ' duct ' usually consisted of a sharp expansion from the entry to the face of the cylinders, so the duct loss was fairly large and roughly inversely proportional to the square of the velocity ratio.

Blade-root losses were high, usually accounting for about half the total. Flared roots, of large chord and moderate thickness, had no advantage, except at low J, over smaller roots of poorer aerodynamic shape.

1.3. *The Propeller Turbine Problem.*—Entry loss in the turbine engine intake results in a decrease of thrust and an increase in specific fuel consumption. Fig. 3, compiled from a few miscellaneous engine performance estimates, shows roughly the effect of entry loss on thrust. A 10 per cent loss of ram leads to 5 per cent loss of thrust at 500 m.p.h. flight speed, and about half the amount at 300 m.p.h. The corresponding increases in specific fuel consumption are somewhat smaller, owing to the decrease in mass flow which accompanies a loss of pressure in the intake. Compared with these figures, the same loss of ram in the entry of a Bristol air-cooled reciprocating engine would increase the internal cooling drag by about 1 lb at 100 ft/sec, *i.e.*, on the average a little over 1 per cent of the total aircraft drag. On this basis, the significance of entry loss has increased with the application to turbine engines.

In the change from air-cooled engine cowl to axial turbine intake, the design conditions of the entry are modified also. Chiefly, since the inlet velocity to the compressor of the turbine engine is high, the entry duct usually has an overall contraction in area, the duct loss is mainly skin friction, and as such is governed more by the velocity at the compressor end than by that at the entry. This means that a smaller entry (lower velocity ratio) can be used, to ensure stable flow over the spinner. On the other hand, the blade-root loss becomes more important, because for a given power the engine has a smaller diameter so that the entry is behind thicker roots.

A sloped entry, illustrated in Fig. 1b is an alternative to the usual forward-facing or vertical type, following a suggestion by McKinnon Wood[2]. The spinner is increased in diameter to form a more continuous contour with the engine cowl, and the duct is swept inwards from the entry : this gives a curved inside wall near the entry, the purpose of which is to induce a suction offsetting the normal adverse pressure gradient across the entry. At the same time the larger spinner covers up more of the thick blade root.

Where the blade-root loss is the largest component, a ducted spinner (Fig. 1c) may be worth the added weight and complication. The idea has been tried out before[3] as a method of obtaining fan cooling for air-cooled engines. As a device for reducing entry loss, its main advantage lies in reducing the velocity over the blade roots by a suitable choice of the annular area. In addition a ducted spinner possesses the general advantages of a nose intake such as high limiting velocity ratio and insensitivity to changes of incidence.

1.4. *Scope of Investigation.*—Model tests of a series of annular intakes were made in the 5-ft Open-Jet Wind Tunnel of the Royal Aircraft Establishment between March, 1946, and January, 1947. Models were based on the layouts of two typical propeller turbine engines with axial

*$q=\frac{1}{2}\rho V^2$ = flight ' ram.'

compressors, the Fedden ' Cotswold '* and the Rolls Royce ' Clyde.' These represented respectively the cases of a small engine (about 30-in. diameter, 1400 effective h.p.) for a medium-speed aircraft cruising at 200 to 300 m.p.h., and a large engine (about 50-in. diameter, 3500 effective h.p.) for a faster aircraft cruising at about 450 m.p.h. The differences in size and speed led to different proportions of annular width to spinner diameter on the models. Various spinner and duct shapes were tested, including in each class both vertical and sloped entries. On the Cotswold model, a second position of the propeller in relation to the entry was tried, this representing fairly closely the intake of the Armstrong-Siddeley ' Mamba ' engine. Although originally a fuller programme had been contemplated, tests with propeller were ultimately confined to the small engine cases, these having relatively the thicker blade roots.

In order to examine the nature of scale effect on the loss of thick blade roots, tests were also made in the 24-ft Wind Tunnel on a full-size ducted nacelle, using the whole available speed range of the tunnel (40 ft/sec to 170 ft/sec). The ' blade roots ' for these tests consisted of a set of plain cylindrical shanks, $7\frac{1}{2}$-in. in diameter, representing an extreme case, and giving a maximum Reynolds number comparable with flight.

Section 2 gives an account of the 5-ft Wind Tunnel tests and results, and section 3 describes the tests in the 24-ft Wind Tunnel. Section 4 contains a survey of the general problem of the annular entry, in which the results are correlated with previous data, and generalised into a form suitable for use on new designs.

2. 5-*ft Wind Tunnel Tests.*—2.1. *Model and Equipment.*—The basic model was a 10-in. diameter ducted nacelle (Figs. 4 and 5), mounted on a spindle wired to the roof and floor of the tunnel. This was supplied with interchangeable nose pieces for the various cases, the scale being taken as 1/3 for the Cotswold entries and 1/5 for the Clyde entries. Inside the body of the nacelle were housed three electric motors, the front one driving the model propeller through an extension shaft and gearbox, and the other two driving contra-rotating fans for regulating the internal flow. Each entry was represented up to the compressor inlet, where it matched up to an expanding annular duct (Fig. 5) enclosing the motors and passing through the fans. Behind the rear motor the annular duct was transformed into a fixed circular exit nozzle.

The internal flow was controlled by the speed of the fans which, when combined with three tunnel speeds (0, 80 and 120 ft/sec), provided a range of representative conditions from ground running to high-speed flight. The flow quantity was obtained from the velocity in the exit nozzle, measured by a single central pitot-tube and a pair of static-pressure tappings (Fig. 5). After an initial calibration, this proved a quick and reliable method, and it was found possible to set the flow accurately to prescribed values.

Total head at the compressor inlet position was measured by means of 8 or 12 small pitot-tubes spaced round the circumference of the duct, each traversing across the width of the annulus. Static-pressure tappings on both the inner and outer walls were used to deduce the velocity distribution, assuming linear gradients across the annulus. To separate the duct and spinner losses, total head was also measured just inside the entry by means of 4 equi-spaced traversing pitots. Details of the positions of the pitot- and static-tubes are given in Fig. 5.

The nozzle pressure difference (up to 32 in. of alcohol) was recorded on a vertical alcohol manometer. All other pressures were measured on a multi-tube alcohol manometer of adjustable slope. Generally the latter was set so that at a tunnel speed of 120 ft/sec a pressure of $\frac{1}{2}\rho V^2$ was equivalent to 10-in. of alcohol.

2.2. *Tests.*—The following eight entry arrangements were tested, entries 1 to 5 being based on the smaller engine (Cotswold) and entries 6 to 8 on the larger (Clyde). The main dimensions are summarised in Table 1.

* A projected engine, subsequently not developed.

Entry 1 (Fig. 6) A vertical entry, approximating to the engine firm's preliminary design. The spinner was of the minimum size required to enclose the propeller boss and mechanism. The entry area was 119 sq in. (full-scale) giving a velocity ratio of 2·1 for cruise at 300 m.p.h. At the compressor inlet the duct area was 66 sq in. Two thick struts in the duct, intended to contain supports and auxiliary equipment, were made removable on the model, so that their effect could be measured.

Entry 2 (Fig. 7) Similar to entry 1, but having the plane of the entry closer to the propeller, and a slightly smaller entry area (velocity ratio for cruise = 2·0). The duct contained only thin supporting struts. This arrangement is similar to the Mamba intake.

Entry 3 (Fig. 7) A sloped entry to compare with entry 1. Anticipating a lower limiting velocity ratio for this type of entry, the entry area was made smaller than that of entry 1, giving a design velocity ratio of 1·4.

Entry 4 (Fig. 8) A vertical entry, comparable with entry 1, designed and tested late in the programme, using provisional results from the earlier tests. The spinner diameter was made as large as possible without increasing the maximum diameter of the nacelle. The entry area was slightly greater than that of entry 1 (velocity ratio for cruise = 2·3). In this way it was hoped to combine low blade-root loss with low duct loss.

Entry 5 (Fig. 8) Entry 4 with a ' conical ' spinner replacing the more conventional ' elliptical ' shape.

Entry 6 (Fig. 9) A vertical entry for the Clyde engine, following the lines of an actual design on a high-speed naval aircraft. Velocity ratio 2·2 for level flight at 450 m.p.h. The duct had an overall contraction in area (249 sq in. at entry to 207 sq in. at compressor) but expanded by nearly 2 : 1 in area over the first half of its length in order to match up to a standard intake duct designed by the engine firm. This gave the double advantage of a low average duct velocity and a sharp contraction round the final bend immediately before the compressor inlet. The principle was applied again in entry 4.

Entry 7 (Fig. 9) Similar to entry 6, but with a duct of almost constant area. Design velocity ratio 2·0.

Entry 8 (Fig. 9) A sloped entry to compare with entries 6 and 7. As before this had a smaller entry area than the corresponding vertical entries (design velocity ratio 1·7).

Entries 1 to 5 were tested both with and without propeller, this being a 1/3-scale model of a de Havilland 3-blader (details in Table 1), cropped to about half the proper diameter. Spinner holes round the roots were fully sealed throughout. Entries 6 to 8 were tested only without propeller.

2.3. *Results and Brief Discussion.*—2.3.1. *Presentation.*—Tables of results are given at the end of the report. Figs. 6 to 9 show total head at the compressor plotted against flow for the chief conditions with each entry. The flow is represented by the velocity ratio at the compressor V/V_c; in this way there is only one value for comparable entries at the same flight condition. Figs. 12 and 13 show the loss coefficient (without propeller) in a suitable analytical form. This form is also used to determine the extrapolation to low values of V/V_c of curves in Figs. 6 to 9. Velocity distributions at the compressor inlet are plotted in Figs. 10 and 11.

2.3.2. *Entries* 1 *and* 2.—Apart from the effect of thick struts in the duct, entries 1 and 2 give practically identical results (Figs. 6 and 7). Entry 2 derives a slight advantage from the shorter spinner and lower operating velocity ratio, but the difference is small. The conclusion is that

fore-and-aft position of the propeller relative to the entry is not of major importance, except perhaps in an extreme case when the two are very close together. This is supported by the results of potential flow tests[4] in an electric tank at Völkenrode, which indicate that the retardation in the free stream, when the velocity ratio at entry is greater than unity, takes place in a very short region ahead of the entry.

Taking an average of comparable results for entries 1 and 2, the mean total head at the compressor, at a velocity ratio corresponding approximately to a 300 m.p.h. cruise condition, is $0 \cdot 75q$. The 25 per cent loss of ram is made up as follow :—

Spinner loss	$0 \cdot 05q$,
Duct loss	$0 \cdot 05q$,
Blade-root loss	$0 \cdot 15q$.

Scale effect would reduce the duct loss to about two-thirds the model value, but would not greatly affect the other components. This is discussed more fully in section 4.

Two thick struts (Fig. 6) in the duct of entry 1, increase the loss of ram by 3 per cent, mainly owing to the higher velocity in the duct when the struts are added. More important, perhaps is the effect of the wake of the struts on the circumferential velocity distribution (Fig. 10).

Results (Tables 2 and 3) with the nacelle inclined at 4 deg and 8 deg to the wind show that, with propeller on, the mean total head at the compressor is reduced at the rate of $0 \cdot 005q$ per degree of incidence. With propeller off, the change is more rapid because a separation develops more readily on the top of the spinner. The effect on distribution at the compressor (propeller on) is small.

2.3.3. *Entry* 3.—Entry 3 (sloped) gives a definitely poorer result than entries 1 and 2 (Fig. 7). Although, owing to the bigger spinner, the blade-root loss is about $0 \cdot 04q$ smaller with the sloped entry, this advantage is more than offset by increases in spinner and duct loss. The former is increased in proportion to the surface area of the spinner (*see* fuller discussion in section 4.1). The increase in duct loss comes from the higher velocity in the early part of the duct. This could be avoided by increasing the entry area, but Fig. 12 shows that at the design velocity ratio of $1 \cdot 4$, the loss coefficient is already rising rapidly ; so that an increase of entry area would result in a breakdown of flow on the spinner.

There is no appreciable gain from the surface pressure gradient specially associated with a sloped entry. It is possible that the principle was not carried far enough, but for the type of entry in question it would be very difficult to obtain a satisfactory duct shape with a greater degree of sloping, so that any gain at the entry, which is problematical, would almost certainly be cancelled out by an increase of loss in the duct.

The velocity distribution across the end of the duct (Fig. 10) is less uniform with the sloped than with the vertical entries.

2.3.4. *Entries* 4 *and* 5.—In the case of entry 4 (Fig. 8) which has the largest spinner of the series, the blade root loss is almost halved : $0 \cdot 08q$ compared with $0 \cdot 15q$ for entry 1. The duct loss is also small, but against these two favourable features, the spinner loss is high. Fig. 12 shows that this is because the design velocity ratio of $2 \cdot 3$ is well in excess of the limiting value for stable flow. On balance, the final total head of the complete entry is only $0 \cdot 02q$ higher than that of entry 1.

It appears from this and the previous results that for a given engine and propeller, only small net changes in total head can be produced by varying the geometry of the entry (spinner diameter, entry area, etc.) ; a decrease in one component of the loss usually being accompanied by an increase in another. To obtain the best compromise in a given case, it is necessary to consider separately the possible variations of each of the component losses. As a general rule, it can be expected that where the blade-root loss is a large proportion of the total, as in the cases so far considered, a large-diameter spinner will give the best result.

The result for entry 5 (Fig. 8) provides the exception to the general conclusions of the last paragraph. With this entry, the total head in the design condition is $0 \cdot 82q$, or $0 \cdot 07q$ higher than for entry 1 ; owing primarily to a marked reduction in blade-root loss produced by the ' conical ' spinner. Instances have been found previously[5,6] in which a local step in the spinner contour produced a similar effect. Without more complete tests, it is not possible to make a strict comparison with the more conventional ' elliptical ' spinner shapes, because at the same J, the effective incidence of the blade root is probably different in the two cases, owing to different pressure distributions on the spinners. The result should be regarded rather as an indication that large changes can be produced by modifying the pressure gradients round the roots. A conical spinner is usually considered impracticable because of the difficulty of avoiding large losses at the blade holes, but if a practical scheme were envisaged, this line of investigation should be taken further.

Another result shown by Fig. 8 is that with entries 4 and 5 a high total head of about $0 \cdot 8q$ is maintained down to quite low velocity ratios. This is in contrast to the earlier results, and is explained by the low average duct velocity of entries 4 and 5, whereby the duct loss, even at low velocity ratios, is only a small proportion of flight dynamic head. Thus at low flight speeds, *e.g.*, on climb, the advantage of entries 4 and 5 becomes more marked.

2.3.5. *Entries* 6, 7 *and* 8.—Entries 6, 7 and 8, based on the Clyde engine, were tested only without propeller. In general, the entry loss (Fig. 9) is greater than for the series of Cotswold entries, the reason being that entries for the larger engine have relatively a greater surface area of spinner (*see* section 4.1 for further discussion). Against this, the blade-root loss would be considerably smaller because the blade sections adjacent to the spinner are thinner. On balance, with the same number of propeller blades, the total entry loss for the bigger engine would be a few per cent lower than that for the smaller.

A comparison of results for entries 6 and 7 shows that the expanding contracting duct of entry 6 gives a small but definite advantage over most of the flight range. This is seen most clearly in Fig. 13. In ground running ($V/V_i = 0$) the position is reversed, owing to a greater tendency for flow separation inside the entry lip with the expanding duct. This effect can be countered by increasing the entry-lip radius (*see* section 4.5).

The results for the sloped entry (entry 8) confirm the previous conclusions from the Cotswold series. Fig. 9 shows the direct comparison with entries 6 and 7, and Fig. 13 demonstrates the lower limiting velocity ratio of the sloped entry, which prevents the use of a larger entry area to reduce the duct loss.

3. 24-*ft Wind-Tunnel Tests.*—3.1. *Details of Experiment.*—For scale effect tests in the 24-ft Wind Tunnel, an annular ducted nacelle of 55-in. diameter was fitted with a set of three plain cylindrical shanks, of diameter $7\frac{1}{2}$ in. (the largest that could be fitted into the existing spinner holes). This was taken to represent the extreme case of a propeller with circular roots. The shanks were tested in two fore-and-aft positions, corresponding to the front and rear positions of a contra-rotating propeller, for which the spinner had been designed. Entry loss was measured by means of a single pitot traverse across the entry annulus. The tests were made over a range of tunnel speeds from 40 to 170 ft/sec, with propeller speeds from 70 to 380 r.p.m. (J varying between $8 \cdot 4$ and $0 \cdot 9$, based on a nominal $17 \cdot 7$-ft diameter), and at a series of values of the velocity ratio (varied by means of a sliding ring at the nacelle exit). The blade-root loss was obtained as the difference in entry loss with ' propeller ' on and off.

3.2. *Results.*—The results are given in full in Tables 9 and 10. In Fig. 14, blade-root loss is plotted against tunnel speed for fixed values of J and velocity ratio ($J = 2 \cdot 0$, $V/V_i = 2 \cdot 0$). With the roots in the forward position, the percentage loss increases rapidly between 60 and 170 ft/sec. In the rear position the effect is small and in the reverse direction. At the highest tunnel speed the loss is roughly the same in both positions. From this it is inferred that the

loss of circular or near-circular roots may vary critically in the region of Reynolds number from 10^5 to 4×10^5, but at higher values a more stable condition appears to be reached. (The Reynolds number for a 3-in. thick root at a forward speed of 300 m.p.h. is approximately 7×10^5). The equivalent drag coefficient of the roots at the highest test speed is of the same order as that obtained in the model tests. This comparison is discussed further in section 4.3.

In addition to the Reynolds number effect, the following results can also be seen from Tables 9 and 10 :—

(*a*) At fixed values of tunnel speed and J, lowering the velocity ratio (*i.e.*, increasing the flow) increases the loss. This is probably because as the flow increases the spinner boundary layer forms a decreasing proportion of the total and hence the mean velocity over the blade root increases with the flow

(*b*) The effect of changing J is very marked below $J = 2$, and in opposite directions, so far as the results go, for the two fore-and-aft positions

(*c*) In general the loss is lower for the front than for the rear position, but at the same time more sensitive to changes of J, velocity ratio, and tunnel speed.

These results reflect the complicated nature of the flow over the roots. In particular, the prominent J effect may be taken to indicate the importance of centrifugal forces in determining the flow pattern. The few tests made are not adequate for a full analysis ; so the conclusions drawn above must be taken as provisional only, and confined to values of J and velocity ratio near the chosen representative values.

4. *General Discussion.*—The following analytical discussion shows how the results of the various tests can be generalised, in a form suitable for estimating losses on new designs. Data from other sources also are used to support and in places extend the analysis.

4.1. *Spinner Loss.*—4.1.1. *Limiting velocity ratio.*—Generally speaking, an entry should be designed so that the limiting velocity ratio for stable spinner flow is not greatly exceeded at the highest level flight speed of the aircraft*. The limiting velocity ratio is a function of the growth of boundary layer on the spinner, and therefore depends primarily on the size of the spinner in relation to the entry. A reasonable generalisation of the model results is obtained (Fig. 15) by plotting the limiting values for the various entries against the non-dimensional parameter lr/A, where l is the length of the spinner, r its maximum radius, and A the entry area. The limiting values are deduced from curves of entry total head plotted from Tables 2 to 7. In cases where the definition is vague (owing to lack of data above the limiting value), reference is made also to the loss-coefficient curves in Figs. 12 and 13, which are obtained from measurements at the end of the duct. These indicate slightly lower limiting values than the entry total-head curves, but from a design standpoint the difference is not important.

Two distinct curves are definable from the model results, entries 1 to 5 having consistently higher limiting ratios than entries 6 to 8. The probable reason for this is a difference in surface condition between the two groups of spinners : whereas those of the first group were uniformly smooth, those of the second had been cut to fit a propeller, previous to testing. The holes were sealed over for the tests, but this inevitably left the surface uneven. The two curves in Fig. 15 are labelled ' smooth ' and ' rough,' the terms being used in this special sense.

No distinction is evident between results for vertical and sloped entries, other than is explained by the different values of lr/A. The sloped entries (3 and 8), with their bigger spinners, have the higher values of lr/A and therefore the lower limiting velocity ratios.

* Since the duct loss normally decreases with increase of entry area (*i.e.*, increase of the velocity ratio), the minimum duct + spinner loss will usually be obtained by choosing an entry area which gives a velocity ratio slightly above the ' limiting ' value.

Results for three air-cooled engine entries, taken from full-scale tests in the 24-ft Wind Tunnel (Refs. 7, 8 and unpublished results) are included in Fig. 15, and conform reasonably well to the model curve for rough spinners. The remaining point, at a very small value of lr/A, comes from ducted-spinner tests forming the second part of the present investigation, and classifies as a smooth spinner.

For estimating a practical case, the curve for rough spinners should be used. The following empirical law gives good agreement with the points :—

$$(V/V_i)_{\text{lim}} = 1 + 1{\cdot}8A/lr \,. \quad .. \quad .. \quad .. \quad .. \quad .. \quad .. \quad .. \quad .. \quad (1)$$

The form is logical inasmuch as it implies a limiting velocity ratio of 1 for an infinitely large spinner, and no limit for an infinitely small one (*i.e.*, pitot-type entry). The curve is shown dotted in Fig. 15.

4.1.2. *Loss in stable flow.*—Under stable flow conditions, *i.e.*, below the limiting velocity ratio, the spinner loss is determined by the quantity of boundary-layer air in relation to the total flow into the entry. The parameter lr/A expresses the size of the spinner non-dimensionally : this could be used to plot curves of spinner loss for specific values of the velocity ratio V/V_i. Going a stage further, by multiplying the size parameter by the velocity ratio, we obtain a representative quantity parameter Vlr/Q (where Q is the total flow into the entry $= AV_i$). In Fig. 16a the results for the eight model entries have been plotted in the form of spinner loss against Vlr/Q, using all the experimental points for which the velocity ratio is below the appropriate limiting value. The ' smooth ' and ' rough ' spinners again give different results, but in each class the generalisation is good. As before, comparable vertical and sloped entries conform to the same curve, the sloped entry having the higher entry loss because of its bigger spinner.

The same analysis has been applied to the results of a series of model tests[9] made at the A.V.A., Göttingen, in which the spinner length and diameter were varied independently. These results are plotted in Fig. 16b. Again the generalisation is good : in this case the single loss curve lies a little below that for rough spinners from Fig. 16a, which result is thought to be consistent with the relative surface condition of the models.

Collected results for full-scale annular entries, with spinner holes sealed, again show good agreement with the model results. In practice, unsealed spinner holes may make an appreciable contribution to the loss, but by using the curve for rough spinners for estimation purposes, this will mostly be allowed for. An empirical law giving a good approximation to the experimental curve is :—

$$\frac{\Delta H_s}{q} = 0{\cdot}028\left(\frac{Vlr}{Q}\right)^{0{\cdot}7} \quad .. \quad .. \quad .. \quad .. \quad .. \quad .. \quad .. \quad .. \quad (2)$$

ΔH_s being the spinner loss.

The further effect of gaps between the spinner surface and the bottom of a flared blade is discussed under blade-root loss (section 4.3).

4.2. *Duct Loss.*—For axial compressors, the form of the duct is relatively simple, involving no sudden changes in area and only moderate curvature. Generally speaking, friction loss predominates over separation loss. Moreover, since the friction accumulates most rapidly near the compressor end of the duct, where the velocity is highest, the loss is not greatly dependent on the nature of the flow ahead of the entry. Under these conditions, the duct loss can be expressed, to a first approximation, by a relation of the form :—

$$\frac{\Delta H_d}{q_c} = C_F I \quad .. \quad .. \quad .. \quad .. \quad .. \quad .. \quad .. \quad .. \quad .. \quad .. \quad (3)$$

where

ΔH_d is duct loss = mean total head at entry minus mean total head at compressor

q_c is mean dynamic head at compressor

C_F is effective skin-friction coefficient,

and I is the value of the following integral, depending only on the geometry of the duct :—

$$I = 2\int_0^L \left(\frac{A_c}{A'}\right)^2 \frac{dx}{r_O - r_I}.$$

In this,

A' is the duct area at any section (A_c is the area at compressor end of duct),

r_O, r_I are the outer and inner radii of annulus,

x is the distance of the section aft of the entry plane, measured along the axis of the engine (L is the total axial length of the duct).

The derivation of relation (3) is given in the Appendix.

Fig. 17 shows the measured duct loss for each of the model entries (using an average value over the range of flow covered in the tests) plotted against the value of I. All the non-expanding ducts conform to a single straight line through the origin, the slope of which therefore determines the effective skin friction coefficient for this group of entries. The value is 0·0077, which compares with about 0·0060 for a flat plate in turbulent flow at the same Reynolds number, based on the length of the duct and the mean duct velocity.

Results for the three expanding-contracting ducts (entries 4, 5 and 6) lie on a second line having a slope of 0·0110. The higher value for these entries is explained partly by the lower Reynolds number (following from the lower duct velocity) and partly by a higher skin-friction coefficient in the expanding portion of the duct. The latter is a general result which has been discussed in recent papers by Tillman[10] and Squire[11]. It should be recalled (section 2.3.5) that despite the higher friction coefficient, the expanding-contracting duct has a smaller actual loss than a comparable non-expanding duct, because of the lower average duct velocity, which is reflected in the smaller value of I.

Following the above analysis, it is suggested that duct loss at full-scale Reynolds numbers can be estimated by means of equation (3), using values of C_F taken from the curves plotted in Fig. 18, according to the type of duct. These curves are respectively 30 per cent and 75 per cent higher than the curve of skin-friction coefficient for a flat plate in turbulent flow.

Fig. 17 includes two points for entry 1, these being obtained from tests with and without the thick internal struts shown in Fig. 6. To the general order of accuracy, the same value of C_F applies to both results, *i.e.*, the extra loss with the struts is entirely accounted for by the change in value of I. In both cases expansions are avoided, *i.e.*, the net area of the duct decreases steadily throughout its length.

4.3. *Blade-Root Loss.*—The tests of model entries 1 to 5 with the same three-bladed propeller cover a considerable range of blade-root thickness and thickness/chord ratio, owing to the different spinner sizes. Excluding entry 5 because of the special effect of the conical spinner, it is found that the blade-root loss is directly proportional to the degree of blockage of the entry, based on the blade-root thickness. This is shown in Fig. 19a, where the loss, expressed as a fraction of free-stream dynamic head is plotted against the non-dimensional parameter $Nt/2\pi R$, in which

N is the number of blades

t maximum thickness of a representative section

R radius of representative section.

The representative section chosen is that at 0·35 of the entry width from the spinner surface : assuming a typical level flight condition in which $V_i = 0 \cdot 7V$, this is the mid-section relative to the flow at the blade-root. The empirical law deduced from the figure is :—

$$\frac{\Delta H_b}{q} = 0 \cdot 7 \frac{Nt}{2\pi R} \quad .. \quad .. \quad .. \quad .. \quad .. \quad .. \quad .. \quad .. \quad .. \quad (4)$$

ΔH_b being the blade-root loss. Expressed otherwise, this means that the loss corresponds to a blade-root drag coefficient of 0·7, based on the thickness of the representative section and on free-stream velocity. No separate effect of thickness/chord ratio is discernible although the t/c of the representative section varies between 80 per cent (entry 1) and 40 per cent (entry 4).

Taking the analysis further, Fig. 19b has been drawn to show results collected from present and past wind-tunnel tests plotted in the same way. Different symbols are used to distinguish between model and full-scale data, and also between roots whose representative t/c is greater or less than 50 per cent. The additional model data confirm the empirical law given by equation (4), the scatter of the points being no greater than could be expected, allowing for the limitations of some of the earlier data. From the smaller number of full-scale results the indications are :—

(*a*) Circular roots give the same result as the models, *i.e.*, the loss is according to equation (4).

(*b*) Roots with thickness/chord ratio between 30 per cent and 50 per cent have a 30 per cent lower loss for the same thickness ; this corresponding to the lower line in Fig. 19b (equivalent drag coefficient 0·5 based on thickness).

Further reduction of the coefficient might be obtained with full-scale roots of still smaller t/c, but on the evidence of the model data (t/c varying between 80 per cent and 20 per cent in Fig. 19b), no large change is to be expected. For the thinnest roots tested, the loss coefficient, allowing for reduction when expressed in terms of chord instead of thickness, is several times greater than the value of C_D for a comparable two-dimensional section at the same Reynolds number. This applies to both model and full-scale results, and is a further indication (others were given in section 3.2) that the flow over the roots is essentially three-dimensional in character. Thus the usual results of chordwise fairing do not apply.

It is important to note also that with flared blade roots in which the chord is increased suddenly as the root emerges from the spinner, an additional loss is normally caused by the necessary gap between the spinner surface and the bottom of the blade. In a few cases which have been measured[6] the loss increment was of the order of $1\frac{1}{2}$ per cent q per blade, for 1 foot root chord length. It follows that in practice a flared root of this type does not normally show any advantage over a more or less circular root of the same thickness, despite the lower coefficient indicated by Fig. 19b. Direct evidence of this has been obtained from 24-ft Wind Tunnel tests on a Hercules engine nacelle[12].

The collection of results in Fig. 19b includes two cases of contra-rotating propellers. In each case the loss is roughly the same as for a single propeller with the same total blockage.

Summarising, it is concluded that, purely from the aspect of entry loss under normal cruising or high-speed conditions, the most important principle of blade-root design is to reduce the actual thickness of the root sections, whilst retaining a small spinner cutout, and avoiding a sudden change in section near the surface. Low thickness/chord ratio is an advantage if it can be achieved without introducing gap effects of the sort described.

4.4. *Additional Loss in Ground Running.*—At zero forward speed, the spinner loss is negligible, while the propeller generally gives a small pressure rise. On the other hand, the duct loss is usually higher than at moderate flight speeds, because the flow, entering from all directions, tends to separate inside the entry lip. The effect is shown by a rise in the curve of loss coefficient as the velocity ratio approaches zero ; this is a consistent feature of the results (Figs. 12 and 13).

Tests by the A.V.A., Göttingen[9] and by Messrs. Rolls Royce[13], mainly on plain circular entries, have shown the additional loss to be a function of the entry-lip radius. In Fig. 20a the additional loss of the present model entries is plotted against the ratio of lip radius to annular width ; and in Fig. 20b this presentation is extended to include the results from Refs. 9 and 12. (For plain circular entries, the annular width becomes the entry radius.) Very satisfactory agreement is obtained between the different sets of results. It is seen that the entries can be classified according as the duct immediately inside the entry is parallel, diverging or converging. Agreement between full-scale and model results is also good.

The general conclusion is that the ratio of lip radius to entry width should be about 0·1 for a parallel duct and 0·15 for a diverging duct. If this is undesirably high (*e.g.*, from the critical Mach number standpoint) a small degree of convergence just inside the entry should preferably be added. An alternative way of achieving this last compromise is to have different radii on the inside and outside of the lip leading edge.

5. *Summary of Conclusions.*—The main conclusions are summarised below.

(*a*) For a small engine (30-in. diameter, effective h.p. about 1400) with a three-bladed propeller and minimum spinner, the model tests give an entry loss, under level flight conditions, of 25 per cent of free-stream dynamic head ; of which 5 per cent is spinner loss, 5 per cent duct loss, and 15 per cent blade-root loss. On a bigger engine (50-in. diameter, effective h.p. about 3500), spinner loss and duct loss tend to be larger and blade-root loss smaller, the estimated total loss for a typical case being a few per cent less than the above. Scale effect on the model results is likely to be small.

(*b*) With a given engine and propeller, and with spinners of roughly elliptical shape, the net change in total head caused by varying spinner diameter, entry area, or distance between propeller and entry, is usually small, a decrease in one component of the loss being accompanied by an increase in another. Generally, if the blade-root loss is a high proportion of the total, a large diameter spinner gives the best result.

(*c*) A sloped entry is not recommended. Both the spinner and duct losses are increased, and the reduction of blade-root loss is not sufficient to offset this.

(*d*) Brief tests with a conical spinner yield promising results. Further model tests should be made of any practical scheme on these lines.

(*e*) The effect of internal struts, of 40 per cent thickness/chord ratio, on the mean total head can be accounted for purely by the change in skin friction, provided that the net duct area decreases continuously along the length of the duct.

(*f*) Blade-root loss depends primarily on the blockage ratio of the blades, based on the actual root thickness. Using the notation :—

ΔH_b blade-root loss

N number of blades

t representative root thickness

R representative root radius

the following empirical law is deduced from the model results :—

$$\frac{\Delta H_b}{q} = \frac{0{\cdot}7Nt.}{2\pi R}$$

Although evidence has been found of a critical Reynolds number region for circular roots, in practice the change in loss between model and full-scale is usually small. To a first approximation, full-scale blade-root loss is given by the same type of law, in which the numerical coefficient is

0·7 for circular or near-circular roots,
0·5 for thin roots ($t/c < 0{\cdot}5$).

(*g*) Spinner loss (Fig. 16) and duct loss (Figs. 17 and 18) can also be expressed in general terms, from the results of the tests.

(*h*) The additional duct loss which occurs in ground running depends on the entry-lip radius and on the shape of the initial part of the duct. Generalised results (Fig. 20) indicate that the ratio of lip radius to entry width should be at least 0·1 for a parallel duct and 0·15 for a divergent duct. Failing this it is desirable to have a small degree of convergence just inside the entry.

Acknowledgments.—Assistance in the experimental work was given by D. J. Harper and D. J. Kettle of the R.A.E.; and also by E. Fraenkel while on vacation from Toronto University.

LIST OF SYMBOLS

General

ρ	Density of air
V	Free-stream velocity
q	Free-stream dynamic head $= \frac{1}{2}\rho V^2$
V_i	Mean velocity at duct entry
q_i	Entry dynamic head $= \frac{1}{2}\rho V_i^2$
V_c	Mean velocity at end of duct, *i.e.*, at entry to compressor
q_c	Dynamic head at end of duct $= \frac{1}{2}\rho V_c^2$
Q	Volume flow
H_c	Mean total head at end of duct, referred to free-stream static
ΔH	Loss of total head up to end of duct or total entry loss
ΔH_s	Loss of total head on spinner
ΔH_d	Loss of total head in duct
ΔH_b	Loss of total head caused by blade roots
ΔH	$= \Delta H_s + \Delta H_d + \Delta H_b = q - H_c$
J	Propeller advance ratio

Sections 4.1 *and* 4.3

l	Distance of nose of spinner forward of entry
r	Maximum radius of spinner
A	Entry area ($AV_i = Q$)
N	Number of propeller blades
t	Representative blade-root thickness
R	Representative blade-root radius
c	Representative blade-root chord

LIST OF SYMBOLS—*continued*

Section 4.2 *and Appendix*

V'	Average duct velocity at arbitrary section
A'	Area of arbitrary section
A_c	Area at end of duct, *i.e.*, at entry to compressor
r_I	Radius of inner surface of arbitrary section
r_O	,, ,, outer ,, ,, ,, ,,
s	Distance along duct, measured along centre-line
x	,, ,, ,, ,, parallel to nacelle axis
L	Total axial length of duct
θ	Inclination of duct centre-line to axis
ΔF	Friction force on duct element
Δp	Pressure drop on duct element
C_F	Effective skin-friction coefficient of duct
I	Duct geometric integral

$$= 2\int_0^L \left(\frac{A_c}{A'}\right)^2 \frac{dx}{(r_O - r_I)}$$

Section 4.4

e	Entry-lip radius
d	Annular width at entry

REFERENCES

No.	*Author*	*Title, etc.*
1	A. S. Hartshorn and L. F. Nicholson ..	Aerodynamics of the cooling of aircraft reciprocating engines. R. & M. 2498. May, 1947.
2	R. McKinnon Wood	The design of side entries to ducts in aircraft. A.R.C. 8528. March, 1945. (Unpublished.)
3	J. Seddon, M. F. Mullins and D. J. Harper	Model tests on the cooling and drag characteristics of two hollow spinner fans, suitable for a radial air-cooled engine or annular ring radiator. R.A.E. Report Aero. 2085. October, 1945.
4	H. Hahnemann and K. Bammert ..	Tests in an electrolytic tank on a ramming and non-ramming air intake for a gas turbine power plant. M.A.P. (Völkenrode) Translation ; R. & T. 182.
5	E. Floyd Valentine	Preliminary investigation directed toward improvement of the N.A.C.A. cowling. N.A.C.A. Advance Restricted Report. A.R.C. 5970. July, 1942. (Unpublished.)
6	Bristol Aeroplane Company	Tests on a $\frac{1}{5}$-scale model of the Buckingham cowl in the R.A.E. small wind tunnels. A.R.C. 9840. March, 1943. (Unpublished.)

REFERENCES—*continued*

No.	*Author*	*Title, etc.*
7	C. Roe	Drag and cooling tests in the 24-ft tunnel on a Centaurus-Buckingham wing nacelle installation. Part I. CTA Exhaust system. R. & M. 2333. July, 1946.
8	T. B. Owen, C. Roe, H. Shaw and B. Stokes	Drag and cooling tests in the 24-ft tunnel on a Centaurus-Buckingham wing nacelle installation. Part III. High speed entry (Tempest type). R. & M. 2333. July, 1946.
9	D. Küchemann and J. Weber ..	Triebwerksverkleidungen (Ringhauben). Göttingen Monograph J_2.
10	W. Tillman	Investigations of some peculiarities of turbulent boundary layers on plates. Reports and Translations No. 45. A.R.C. 9732. March, 1946. (Unpublished.)
11	H. B. Squire	Experiments on conical diffusers. R. & M. 2751. November, 1950.
12	L. F. Nicholson and H. Shaw	24-ft tunnel tests on the cowl entry losses on a Hercules-Beaufighter nacelle fitted with flared and unflared propellers. A.R.C. 8802. May, 1945. (Unpublished.)
13	F. R. Murray and W. J. Annand ..	*Meteor* Air Intake: wind-tunnel tests on quarter-scale models of existing and improved intakes. Rolls Royce Experimental Department Report. Dor/Chr/WJA.1/BFM. July, 1947.

APPENDIX

Expression for Duct Loss in Terms of Effective Skin-Friction Coefficient

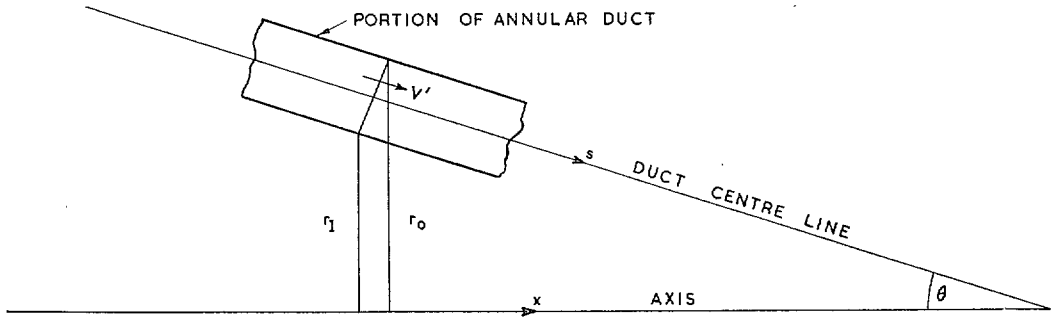

Consider the above diagram. The friction force on a duct element, in the direction of flow, is approximately

$$\Delta F = \tfrac{1}{2}\rho V'^2 \,.\, C_F \,.\, 2\pi(r_I + r_o)\, ds$$

where ds = element of length along duct centre-line. Assuming complete mixing at every stage this force gives rise to a pressure drop

$$\Delta p = \Delta F/A',$$

A' being the duct cross-sectional area. The drop in *total head* through the length of the duct is given approximately by the sum of these pressure drops,

$$\Delta H_d = \int_s \Delta F/A'.$$

Writing the loss in terms of the dynamic head at the end of the duct, q_c we have

$$\frac{\Delta H_d}{q_c} = \int \left(\frac{V'}{V_c}\right)^2 \frac{2\pi(r_I + r_O)}{A'} C_F \, ds.$$

By continuity, $A'V' = A_cV_c$. Hence

$$\frac{\Delta H_d}{q_c} = \int \left(\frac{A_c}{A'}\right)^2 \frac{2\pi(r_I + r_O)}{A'} C_F \, ds.$$

Since $A' = \pi(r_O^2 - r_I^2)$ sec θ, and $ds = dx$ sec θ, this may be written

$$\frac{\Delta H_d}{q_c} = \int \left(\frac{A_c}{A'}\right)^2 \frac{2C_F \, . \, dx}{(r_O - r_I)} .$$

Assuming C_F constant, and writing L for the total axial length of the duct, we have, finally,

$$\frac{\Delta H_d}{q_c} = 2C_F \int_0^L \left(\frac{A_c}{A'}\right)^2 \frac{dx}{(r_O - r_I)} = C_F.I.$$

TABLE 1

Model Dimensions (5-ft Wind Tunnel Tests)

Diameter of nacelle	10 in. actual size
Overall length of nacelle (with entry 1)	65 in. ,, ,,
Diameter of exit nozzle	2 in. ,, ,,
Entries 1 to 5 (dimensions full-scale) :—	
Scale	$\frac{1}{3}$
Annular area at end of duct (*i.e.*, at compressor inlet) A_e	65·7 sq in.
Diameter of cropped propeller	5 ft
Number of blades, N	3
Type	de Havilland flared
Assumed air consumption for cruise (300 m.p.h.)	180 cu ft/sec

	1	2	3	4	5	
Entry area, A	119	113	82	132	132	sq in.
Length of spinner, l	30·5	26·4	33·3	26·2	26·2	in.
Max. radius of spinner, r	8·2	8·2	11·4	11·9	11·9	in.
Thickness of propeller blade at representative section ahead of entry, t	4·2	4·2	3·2	2·6	3·1	in.
Thickness/chord at representative section	0·82	0·82	0·57	0·40	0·55	—
Radius of representative section	8·4	8·4	10·1	11·9	10·3	in.
Axial length of duct, L	17·4	17·4	14·4	21·7	21·7	in.
Entry lip radius, e	$\frac{3}{8}$	$\frac{3}{8}$	$\frac{3}{10}$	$\frac{3}{10}$	$\frac{3}{10}$	in.

Entries 6 to 8 (dimensions full-scale) :—	
Scale	$\frac{1}{5}$
Annular area at end of duct	207 sq in.
Assumed air consumption for level flight (450 m.p.h.)	525 cu ft/sec

	6	7	8	
Entry area, A	249	222	196	sq in.
Length of spinner, l	40·3	40·3	49·8	in.
Max. radius of spinner, r	15·3	15·3	19·5	in.
Axial length of duct, L	31·3	31·3	23·6	in.
Entry lip radius, e	$\frac{5}{8}$	$\frac{3}{4}$	$\frac{3}{4}$	in.

TABLE 2

Results for Entry 1

Tunnel V ft/sec	Blade angle at 42-in. rad	J	Flow $\frac{V}{V_i}$	Flow $\frac{V}{V_e}$	Swirl at end of duct (deg)	Mean total head $\div q$ at entry	Mean total head $\div q$ at end of duct	Total-head loss $\div q_i$ up to entry	Total-head loss $\div q_i$ up to end of duct
$\alpha = 0$ deg : no propeller : all struts in :—									
120			2·48	1·37		0·907	0·853	0·448	0·902
,,			2·01	1·11		0·947	0·876	0·213	0·498
,,			1·66	0·92		—	0·857	—	0·395
80			1·42	0·79		0·964	0·812	0·073	0·380
,,			1·18	0·65		0·979	0·736	0·029	0·367
,,			1·00	0·55		0·979	0·652	0·021	0·346
0			0	0		—	—	0	0·40
$\alpha = 4$ deg : no propeller : all struts in :—									
120			2·01	1·11		—	0·844	—	0·625
80			1·42	0·79		—	0·762	—	0·483
80			1·00	0·55		—	0·585	—	0·414
$\alpha = 8$ deg : no propeller : all struts in :—									
120			2·01	1·11		—	0·797	—	0·820
80			1·42	0·79		—	0·700	—	0·608
80			1·00	0·55		—	0·534	—	0·465
$\alpha = 0$ deg : no propeller : thick struts removed :—									
120			2·01	1·11		0·930	0·899	0·281	0·406
80			1·42	0·79		0·956	0·864	0·089	0·274
$\alpha = 0$ deg : with propeller : all struts in :—									
120	42 deg	1·69	2·48	1·37	1	0·792	0·736		
,,	,,	,,	2·01	1·11		0·818	0·696		
,,	,,	,,	1·66	0·92		0·827	0·640		
,,	,,	1·24	2·01	1·11		0·812	0·687		
,,	,,	,,	1·66	0·92		0·805	0·643		
80	,,	,,	1·25	0·69	1	0·796	0·537		
,,	,,	0·80	1·66	0·92	1	0·892	0·735		
,,	,,	,,	1·25	0·69		0·902	0·629		
,,	,,	,,	1·00	0·55		0·916	0·492		
0	25 deg	0	0	0		—	—	—0·25	+0·24
,,	,,	0	0	0		—	—	—0·17	0·30
$\alpha = 0$ deg : with propeller : thick struts removed :—									
120	42 deg	1·69	2·48	1·37		0·785	0·735		
,,	,,	1·24	2·48	1·37		0·806	0·741		
80	,,	1·24	1·25	0·69		0·810	0·658		
,,	,,	0·80	1·25	0·69		0·886	0·747		
$\alpha = 8$ deg : with propeller : all struts in :—									
80	42 deg	1·24	1·66	0·92			0·626		
,,	,,	1·24	1·25	0·69			0·495		
,,	,,	0·79	1·25	0·69			0·563		
,,	,,	0·79	1·00	0·55			0·455		

TABLE 3

Results for Entry 2

Tunnel V ft/sec	Blade angle at 42-in. rad.	J	Flow $\frac{V}{V_i}$	Flow $\frac{V}{V_e}$	Swirl at end of duct (deg)	Mean total head ÷ q: at entry	Mean total head ÷ q: at end of duct	Total-head loss ÷ q_i: up to end of duct
α = 0 deg : with propeller : all struts in :—								
120	42 deg	1·70	2·36	1·37	—4	0·816	0·774	
,,	,,	,,	1·91	1·11	—3	0·808	0·769	
,,	,,	,,	1·58	0·92	—2	0·790	0·737	
,,	,,	1·24	1·91	1·11	—2	0·832	0·776	
,,	,,	,,	1·58	0·92	—2	0·820	0·764	
80	,,	,,	1·20	0·69	—1	0·812	0·670	
,,	,,	0·80	1·58	0·92	—1	0·864	0·809	
,,	,,	,,	1·20	0·69	—1	0·885	0·746	
,,	,,	,,	0·95	0·55	0	0·897	0·638	
α = 8 deg : with propeller : all struts in :—								
80	42 deg	1·25	1·20	0·69			0·629	
,,	,,	0·80	1·19	0·69			0·650	
,,	,,	0·80	0·95	0·55			0·644	
α = 0 deg : no propeller : all struts in :—								
120	—		2·36	1·37		—	0·881	0·660
,,			1·89	1·11		0·955	0·896	0·372
,,			1·58	0·92		0·966	0·881	0·296
80			1·19	0·69		0·960	0·813	0·264
α = 0 deg : with propeller : struts on vertical centre-line removed :—								
120	42 deg	1·71	1·89	1·11		0·814	0·765	
120	,,	1·25	1·89	1·11		0·817	0·752	
80	,,	1·25	1·19	0·69		0·781	0·649	
80	,,	0·80	1·19	0·69		0·861	0·710	

TABLE 4

Results for Entry 3

Tunnel V ft/sec	Blade angle at 42-in. rad.	J	Flow $\frac{V}{V_i}$	Flow $\frac{V}{V_e}$	Swirl at end of duct (deg)	Mean total head ÷ q at entry	Mean total head ÷ q at end of duct	Total-head loss ÷ q_i up to entry	Total-head loss ÷ q_i up to end of duct
$\alpha = 0$ deg : no propeller :—									
120			1·71	1·37		0·936	0·806	0·186	0·565
,,			1·38	1·11		0·945	0·808	0·105	0·365
,,			1·14	0·92		0·948	0·786	0·068	0·279
80			0·98	0·79		0·952	0·725	0·046	0·264
,,			0·86	0·69		0·963	0·691	0·028	0·230
,,			0·69	0·55		0·978	0·553	0·010	0·212
0			0	0					0·27
$\alpha = 0$ deg : with propeller :—									
120	42 deg	1·70	1·71	1·37	−6	0·787			
,,	,,	,,	1·38	1·11	−5	0·794			
,,	,,	,,	1·14	0·92	−4	0·815			
,,	,,	1·25	1·38	1·11	−2	0·811			
,,	,,	,,	1·14	0·92	−2	0·827			
80	,,	,,	0·86	0·69	−2	0·823			
,,	,,	0·80	1·14	0·92	+8	0·995			
,,	,,	,,	0·86	0·69	6	1·016			
,,	,,	,,	0·69	0·55	4	1·021			
$\alpha = 0$ deg : with propeller :—									
120	54 deg	1·70	1·71	1·37	−2	0·830	0·694		
,,	,,	,,	1·38	1·11	−1	0·830	0·696		
,,	,,	,,	1·14	0·92	−1	0·847	0·674		
,,	,,	1·25	1·38	1·11	+3	0·897	0·755		
,,	,,	,,	1·14	0·92	2	0·919	0·738		
80	,,	,,	0·86	0·69	2	0·944	0·651		
,,	,,	0·80	1·14	0·92	6	1·041	—		
,,	,,	,,	0·86	0·69	6	1·072	—		
,,	,,	,,	0·69	0·55	7	1·095	—		

TABLE 5

Results for Entry 4

Tunnel V ft/sec	Blade angle at 42-in. rad.	J	Flow		Mean total head ÷ q		Total-head loss ÷ q_i	
			$\frac{V}{V_i}$	$\frac{V}{V_e}$	at entry	at end of duct	up to entry	up to end of duct
$\alpha = 0$ deg : dash indicates no propeller :—								
120	—	—	2·74	1·37	0·846	0·836	1·157	1·232
,,	—	—	2·21	1·10	0·894	0·857	0·520	0·701
,,	—	—	1·83	0·92	0·934	0·857	0·223	0·482
80	—	—	1·57	0·78	0·937	0·848	0·156	0·376
,,	—	—	1·38	0·69	0·957	0·853	0·082	0·280
,,	—	—	1·10	0·55	0·990	0·823	0·012	0·214
0	—	—	0	0				0·347
120	53½ deg	1·70	2·74	1·37	0·774	0·716		
120	53½ deg	1·70	1·83	0·92	0·837	0·772		
80	53½ deg	1·70	1·38	0·69	0·876	0·784		
80	53½ deg	1·25	1·38	0·69	0·946	0·849		

TABLE 6

Results for Entry 5

Tunnel V ft/sec	Blade angle at 42 in. radius	J	Flow		Mean total head ÷ q		Total-head loss ÷ q_i	
			$\frac{V}{V_i}$	$\frac{V}{V_e}$	at entry	at end of duct	up to entry	up to end of duct
$\alpha = 0$ deg : dash indicates no propeller :—								
120	—	—	2·74	1·37	0·864	0·802	1·022	1·488
,,	—	—	2·21	1·10	0·906	0·831	0·462	0·829
,,	—	—	1·83	0·92	0·945	0·861	0·185	0·468
80	—	—	1·57	0·78	0·932	0·830	0·168	0·420
,,	—	—	1·38	0·69	0·957	0·848	0·082	0·290
,,	—	—	1·10	0·55	0·998	0·847	0·002	0·186
0	—	—	0	0				0·306
120	55 deg	1·70	2·74	1·37	0·876	0·778		
120	55 deg	1·70	1·83	0·92	0·949	0·838		
80	55 deg	1·70	1·38	0·69	0·983	0·840		
80	55 deg	1·25	1·38	0·69	1·063	0·926		

TABLE 7

Results for Entries 6, 7 and 8

Tunnel V ft/sec	Flow		Mean total head ÷ q		Total-head loss ÷ q_i	
	$\frac{V}{V_i}$	$\frac{V}{V_e}$	at entry	at end of duct	up to entry	up to end of duct
Entry 6 : $\alpha = 0$ deg :—						
120	2·44	2·02	—	0·802	—	1·177
,,	1·96	1·63	0·856	0·835	0·564	0·638
,,	1·66	1·38	0·920	0·850	0·212	0·416
,,	1·24	1·03	0·946	0·867	0·082	0·205
80	0·99	0·83	0·942	0·808	0·057	0·188
0	0	0			0	0·250
Entry 7 : $\alpha = 0$ deg :—						
120	2·18	2·02	—	0·808	—	0·910
,,	1·49	1·38	0·930	0·836	0·156	0·365
,,	1·11	1·03	0·943	0·787	0·070	0·263
0	0	0			0	0·225
Entry 8 : $\alpha = 0$ deg :—						
120	1·92	2·02	—	0·691	—	1·135
,,	1·54	1·63	0·860	0·762	0·333	0·568
,,	1·31	1·38	0·893	0·788	0·185	0·366
,,	0·98	1·03	0·899	0·764	0·097	0·226
80	0·79	0·83	0·922	0·689	0·048	0·192
0	0	0			0	0·152

TABLE 8

Nacelle Dimensions (24-ft. Wind Tunnel Tests)

Diameter of nacelle	55·0 in.
Entry inner diameter	27·0 in.
Entry outer diameter	36·0 in.
Spinner diameter at front prop. position	25·0 in.
,, ,, ,, rear ,, ,,	27·0 in.
Distance of front position ahead of entry	21·4 in.
,, ,, rear ,, ,, ,, ,,	6·4 in.
Diameter (*i.e.*, thickness) of cylindrical blades	7·5 in.
Propeller diameter used to calculate J	17·7 ft

TABLE 9

Results for Cylindrical Blades in Front Position

Tunnel V ft/sec	Prop. speed r.p.m.	J	$\frac{V}{V_i}$	Entry total head $\div q$	Total head without prop. at same V/V_i	Blade-root loss $\div q$
40	68	2·0	1·85	0·877	0·940	0·063
,,	,,	,,	1·24	0·885	0·978	0·093
,,	,,	,,	1·09	0·857	0·987	0·130
,,	90	1·5	1·94	0·893	0·934	0·041
,,	,,	,,	1·24	0·921	0·978	0·057
,,	,,	,,	1·09	0·892	0·987	0·095
60	101	2·0	1·88	0·872	0·938	0·066
,,	,,	,,	1·25	0·911	0·978	0·067
,,	136	1·5	1·89	0·878	0·937	0·059
,,	,,	,,	1·27	0·900	0·977	0·077
100	68	4·95	1·19	0·731	0·981	0·250
,,	169	2·0	1·97	0·788	0·932	0·144
,,	,,	,,	1·35	0·817	0·972	0·155
,,	,,	,,	1·18	0·808	0·982	0·174
,,	225	1·5	1·95	0·810	0·933	0·123
,,	,,	,,	1·36	0·831	0·970	0·139
,,	,,	,,	1·17	0·841	0·982	0·141
,,	382	0·89	1·11	0·975	0·986	0·011
170	68	8·45	1·30	0·699	0·974	0·275
,,	225	2·55	1·26	0·765	0·978	0·213
,,	287	2·0	2·29	0·755	0·916	0·161
,,	,,	,,	1·43	0·779	0·966	0·187
,,	,,	,,	1·27	0·790	0·977	0·187
,,	382	1·5	2·30	0·798	0·915	0·117
,,	,,	,,	1·42	0·826	0·966	0·140
,,	,,	,,	1·26	0·825	0·977	0·152

TABLE 10

Results for Cylindrical Blades in Rear Position

Tunnel V ft/sec	Prop. speed r.p.m.	J	$\frac{V}{V_i}$	Entry total head $\div q$	Total head without prop. at same V/V_i	Blade-root loss $\div q$
40	68	2·0	1·84	0·733	0·941	0·208
,,	,,	,,	1·21	0·735	0·980	0·245
,,	,,	,,	1·09	0·724	0·987	0·263
,,	90	1·5	1·93	0·656	0·935	0·279
,,	,,	,,	1·22	0·712	0·979	0·267
,,	,,	,,	1·09	0·722	0·987	0·265
60	101	2·0	1·80	0·732	0·943	0·211
,,	,,	,,	1·19	0·749	0·981	0·232
,,	,,	,,	1·09	0·761	0·987	0·226
,,	136	1·5	1·98	0·700	0·932	0·232
,,	,,	,,	1·23	0·715	0·979	0·264
,,	,,	,,	1·09	0·725	0·987	0·262
100	169	2·0	2·00	0·748	0·930	0·182
,,	,,	,,	1·28	0·741	0·976	0·235
,,	,,	,,	1·10	0·766	0·987	0·221
,,	225	1·5	2·16	0·698	0·922	0·224
,,	,,	,,	1·30	0·712	0·975	0·263
,,	,,	,,	1·09	0·720	0·987	0·267
170	287	2·0	2·22	0·753	0·919	0·166
,,	,,	,,	1·32	0·775	0·973	0·198
,,	,,	,,	1·15	0·788	0·984	0·196
,,	382	1·5	2·20	0·715	0·919	0·204
,,	,,	,,	1·34	0·735	0·971	0·236
,,	,,	,,	1·16	0·750	0·984	0·234

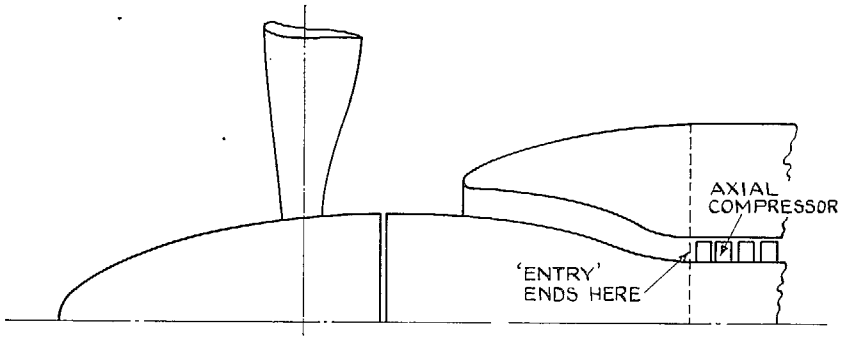

(a) CONVENTIONAL OR 'VERTICAL' ENTRY

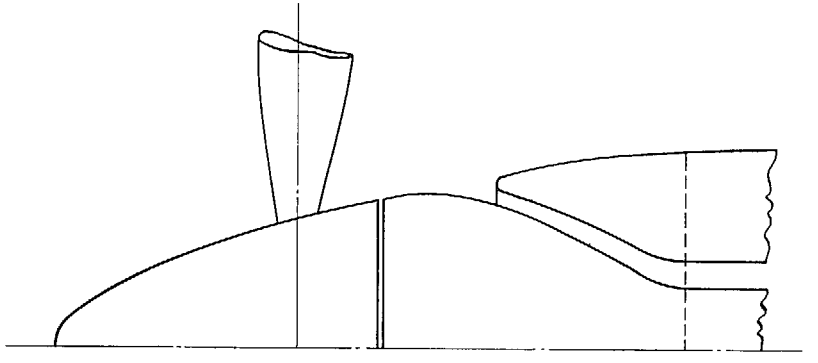

(b) 'SLOPED' ENTRY

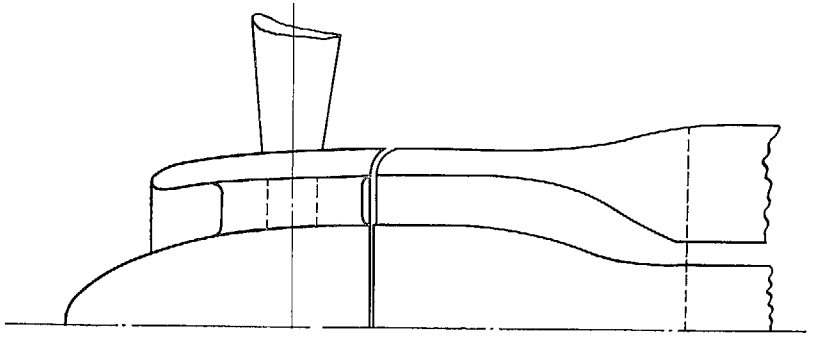

(c) DUCTED SPINNER

FIG. 1. Typical propeller turbine entries.

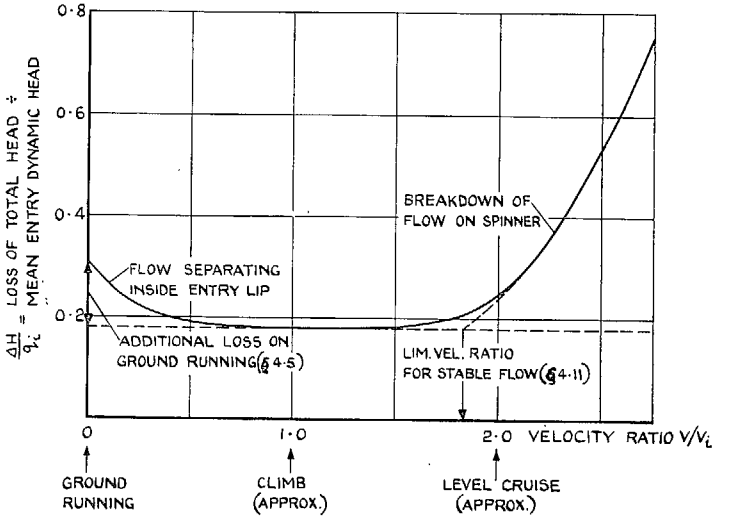

FIG. 2. Typical loss coefficient of annular entry without propeller.

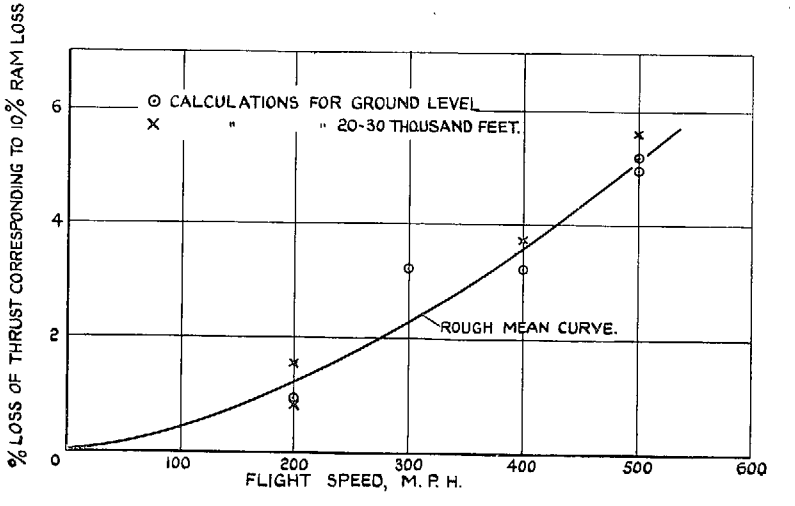

FIG. 3. Collected estimates of effect of entry loss on thrust of a turbine engine.

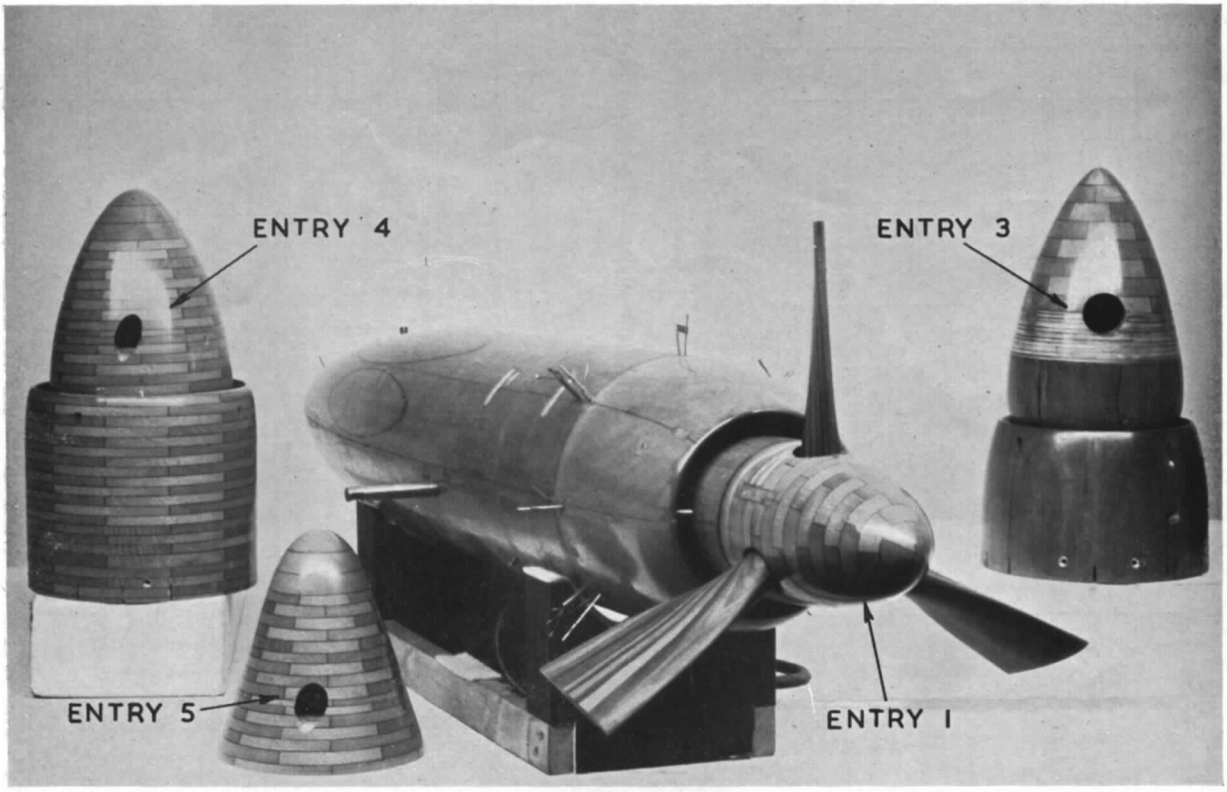

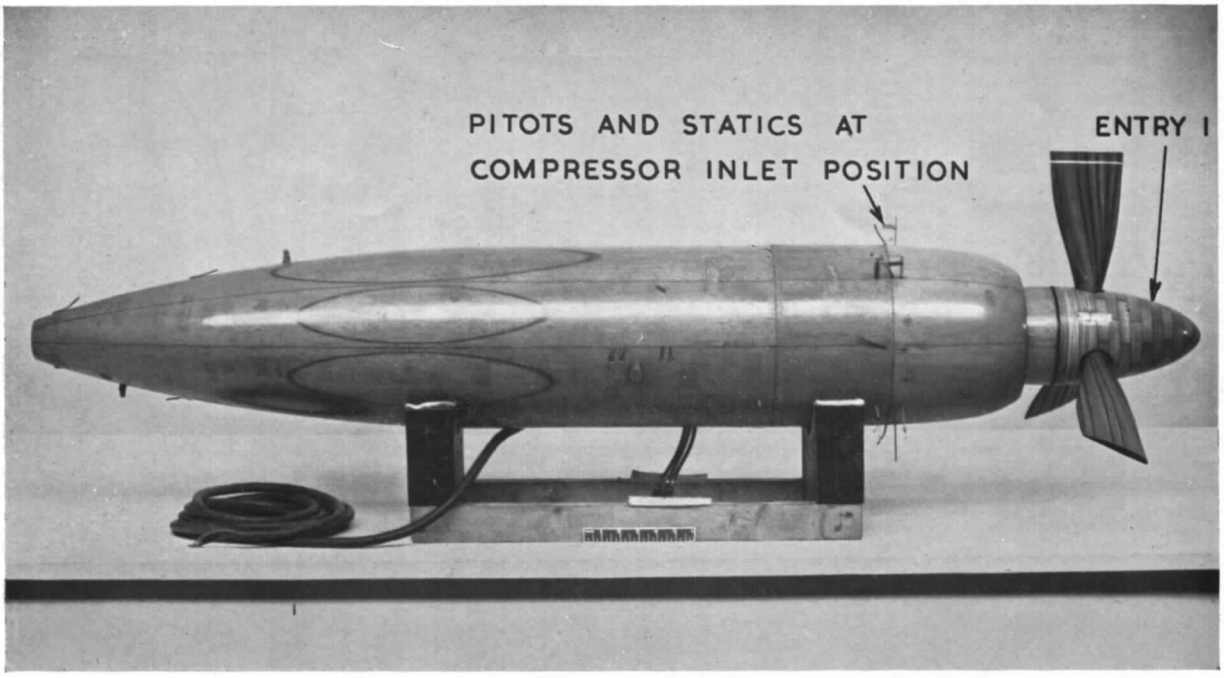

FIG. 4. Model nacelle with alternative entries.

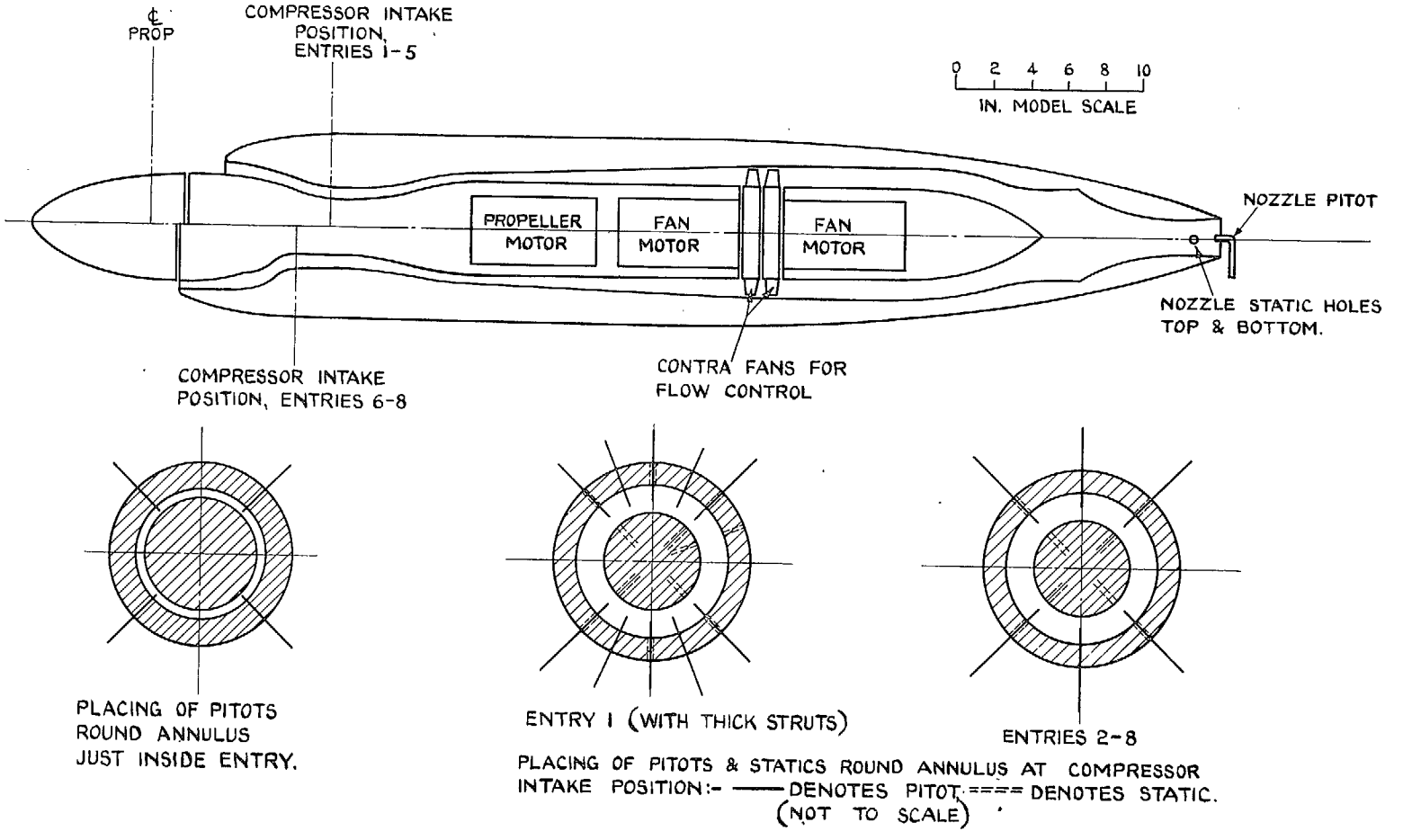

FIG. 5. General arrangement of model nacelle.

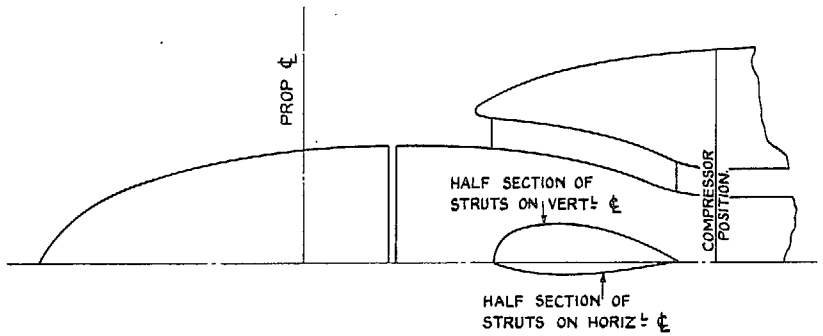

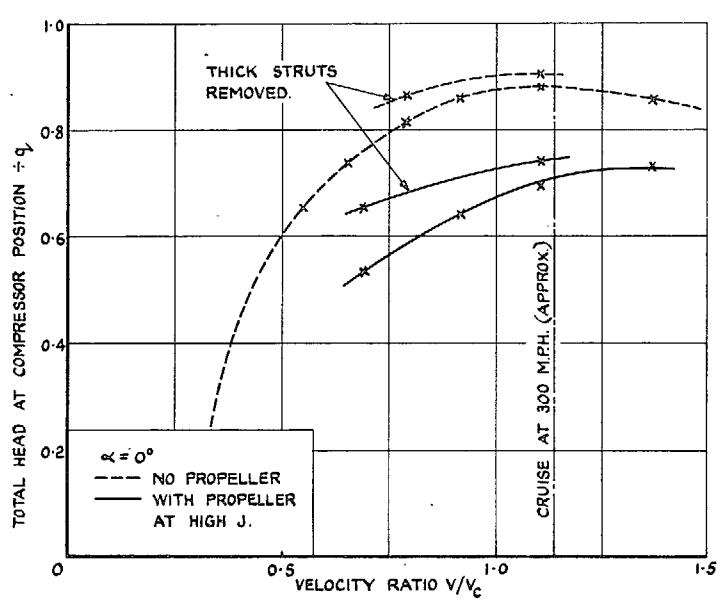

FIG. 6. Entry 1 (Cotswold): with results.

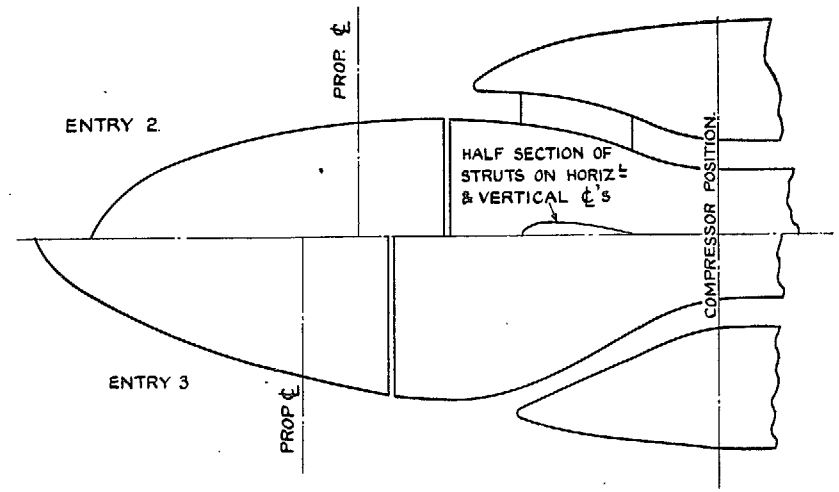

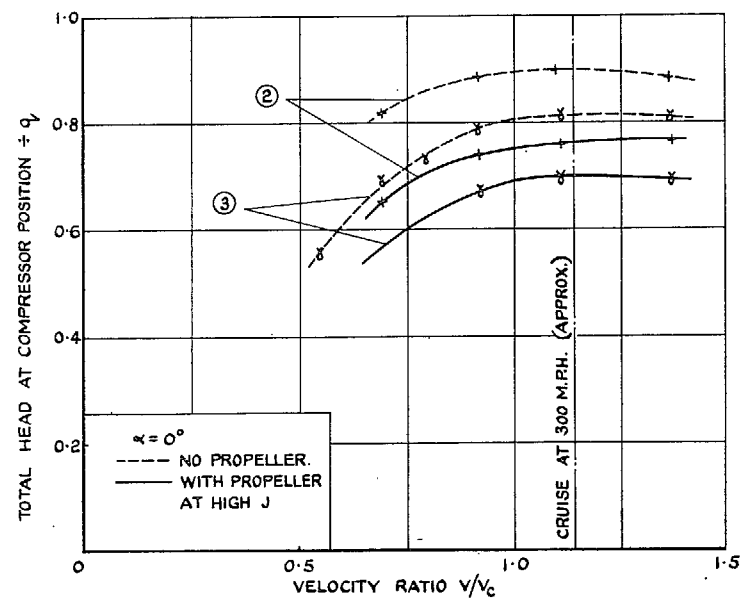

FIG. 7. Entries 2 and 3 (Cotswold): with results.

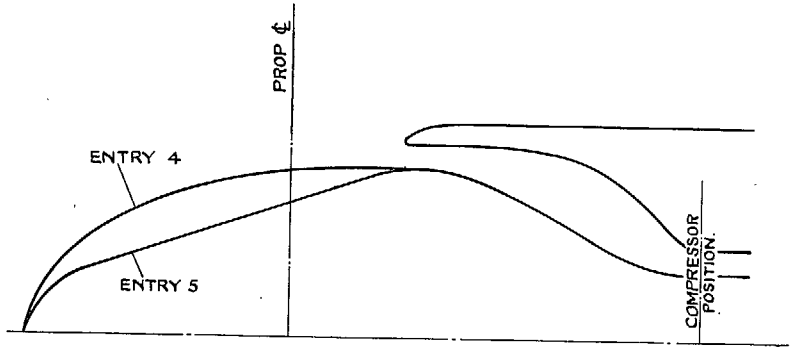

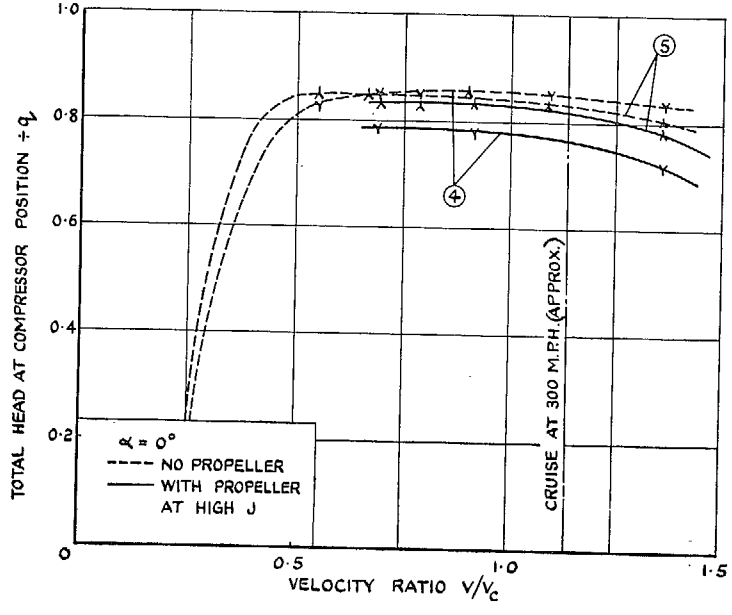

FIG. 8. Entries 4 and 5 (Cotswold) : with results

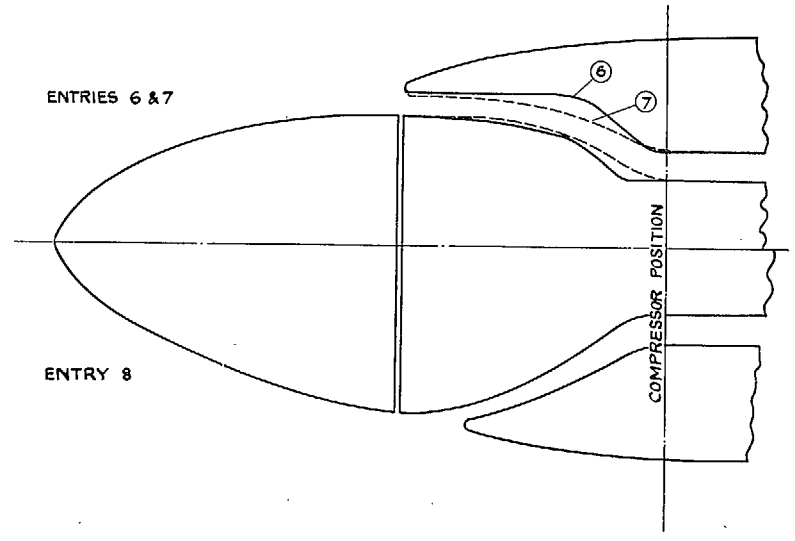

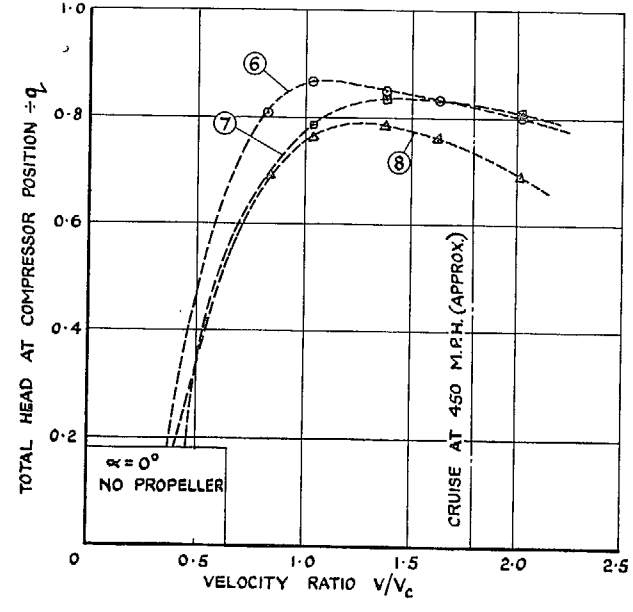

FIG. 9. Entries 6, 7 and 8 (Clyde) : with results.

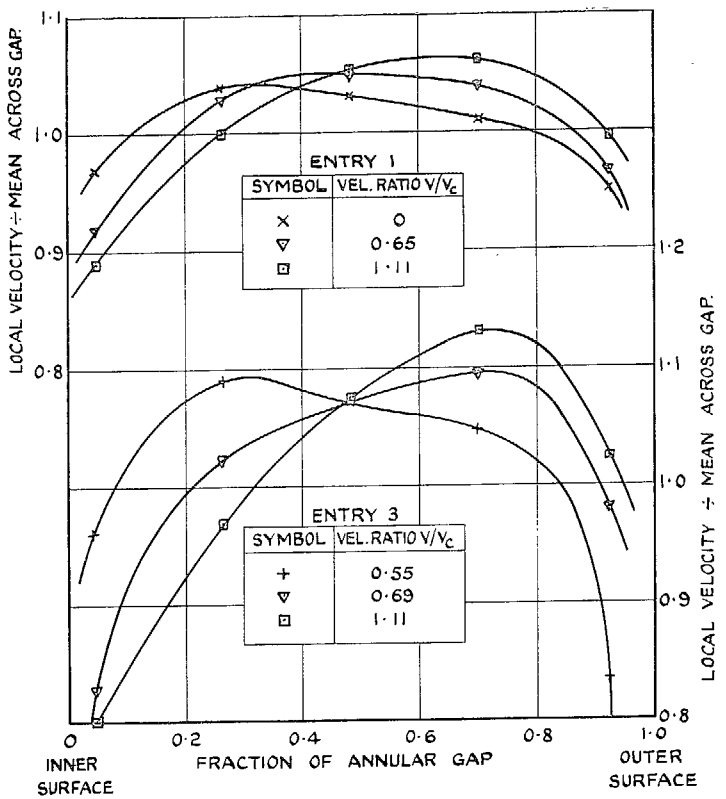

(a) RADIAL DISTRIBUTIONS

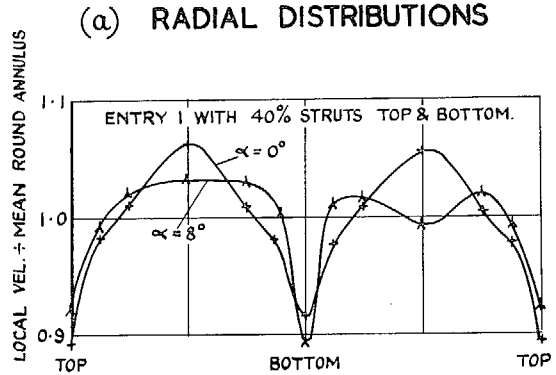

(b) CIRCUMFERENTIAL SHOWING EFFECT OF STRUTS AND OF INCIDENCE

FIG. 10. Velocity distributions at end of duct (entries 1 and 3).

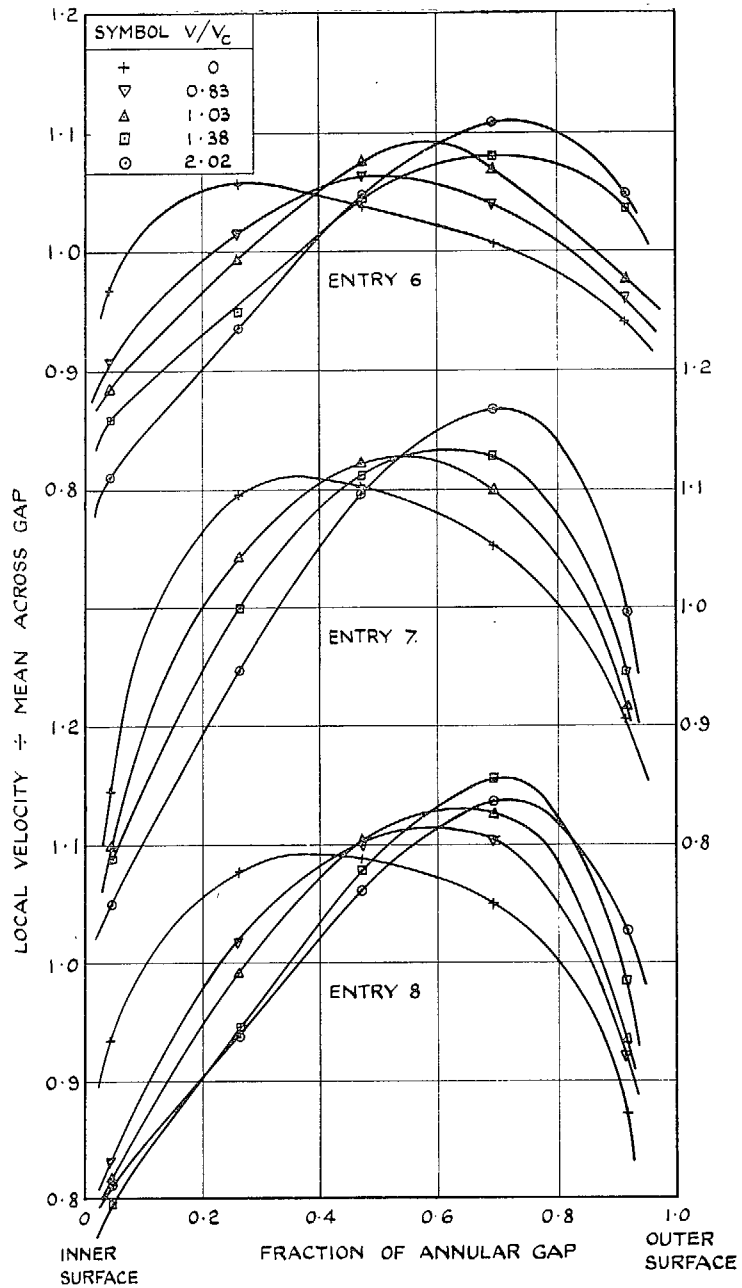

FIG. 11. Velocity distributions at end of duct (entries 6, 7 and 8).

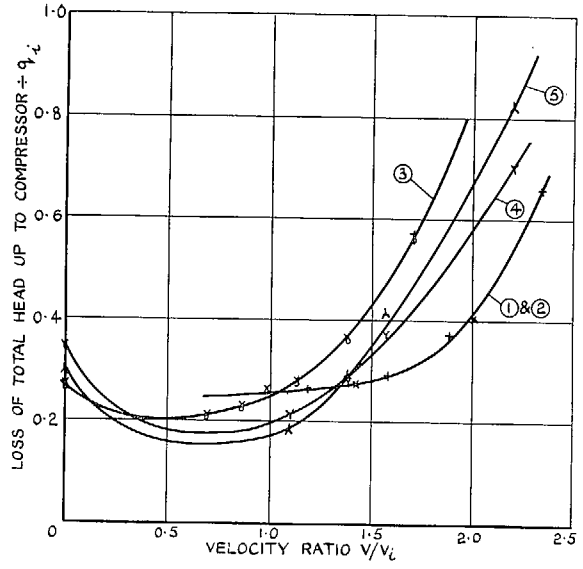

FIG. 12. Entries 1 to 5.

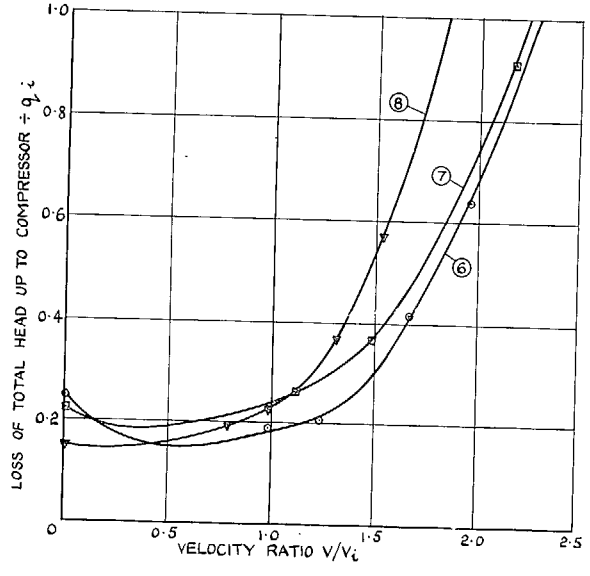

FIG. 13. Entries 6 to 8.

FIG. 12 and 13. Loss coefficients without propeller.

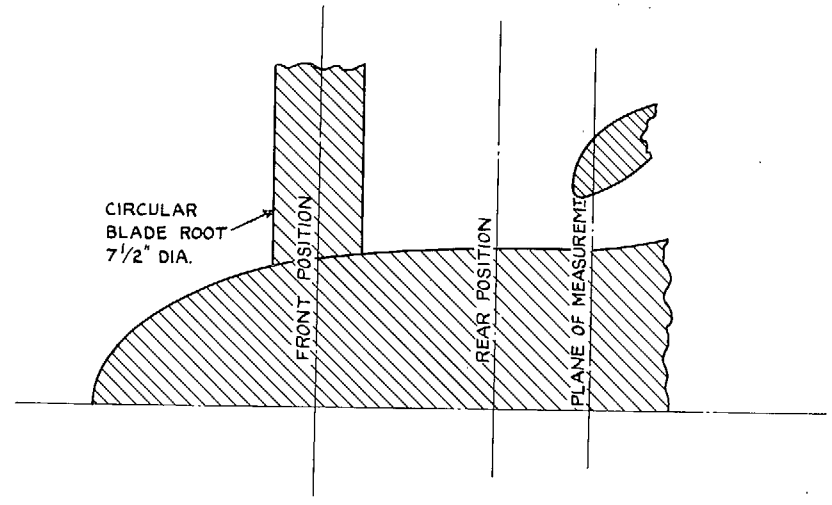

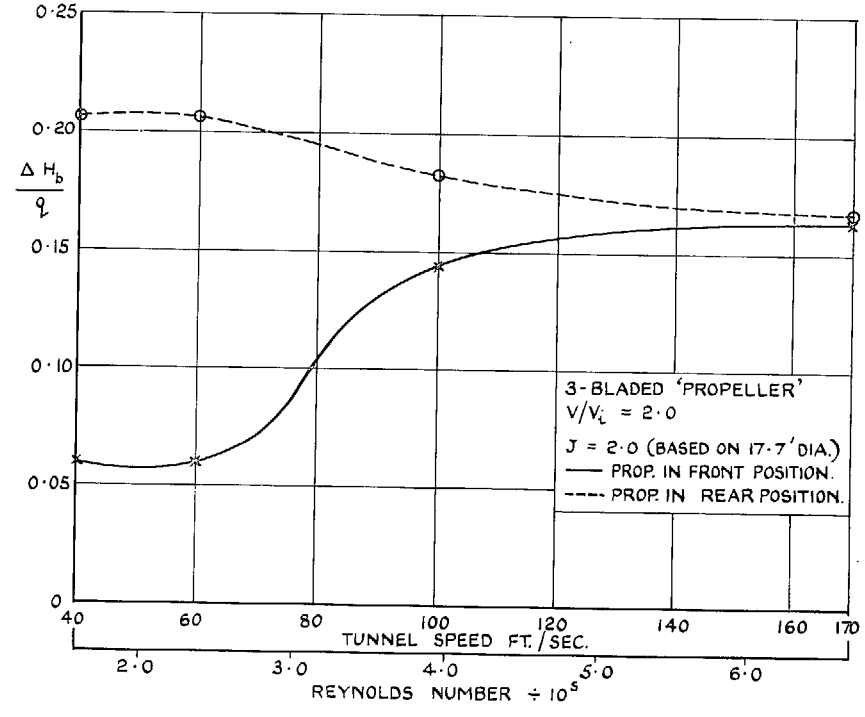

FIG. 14. Loss from circular blade roots at typical flow ratio and J (24-ft Tunnel tests).

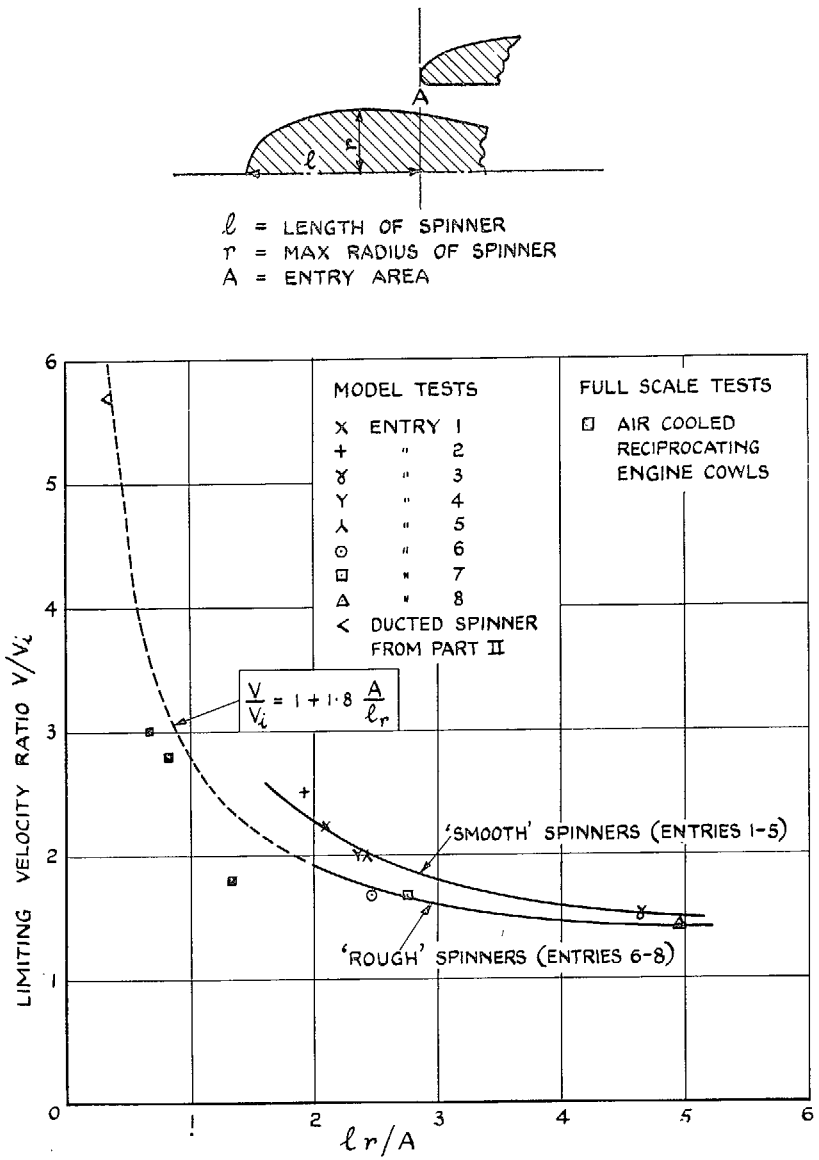

FIG. 15. Spinner loss : limiting velocity ratio for stable flow.

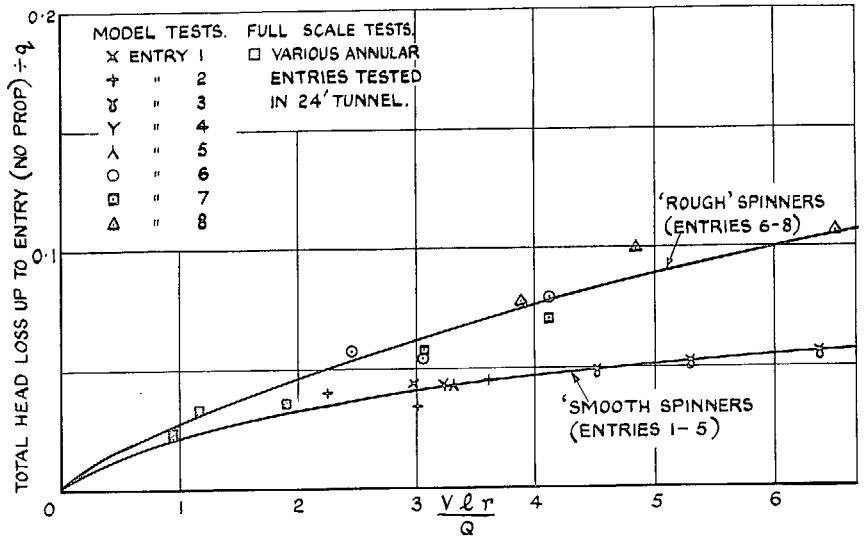

(a) MODEL RESULTS.

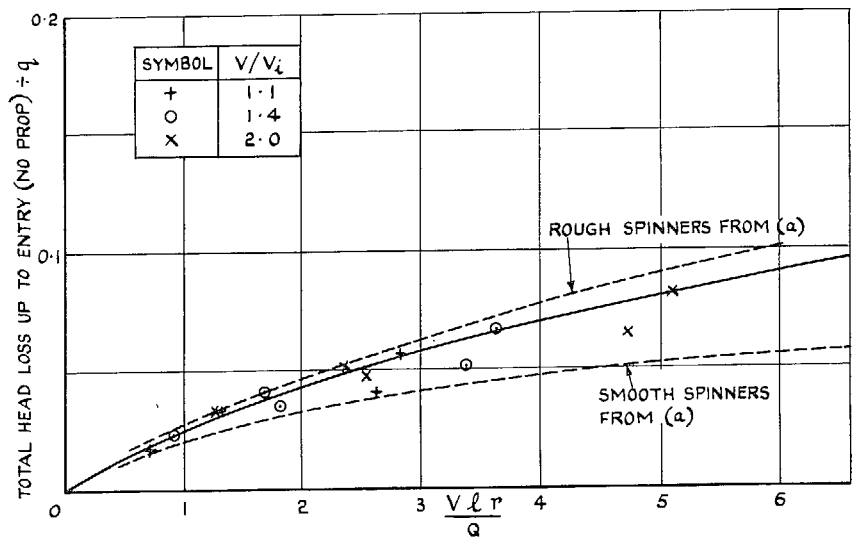

(b) ANALYSIS OF GÖTTINGEN MODEL TESTS (REF. 9.)

FIG. 16. Spinner loss, stable flow.

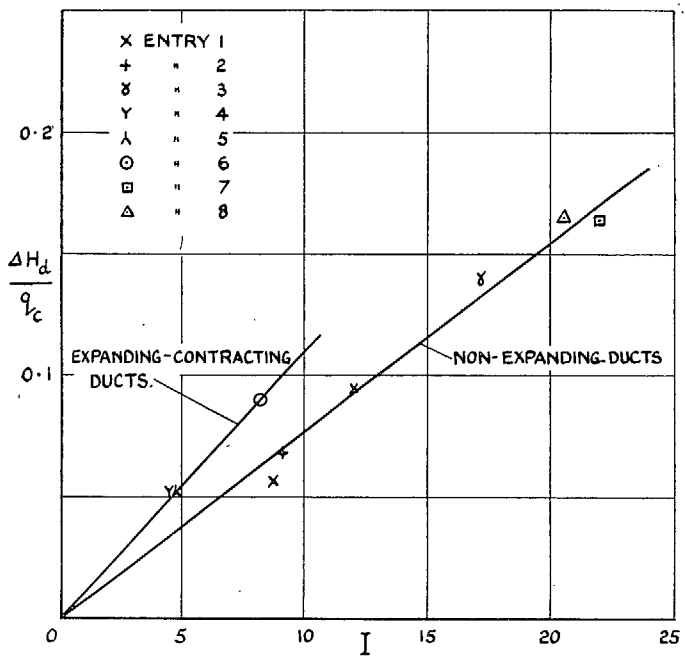

FIG. 17. Average duct-loss coefficient *vs.* integral I (*see* section 4.2).

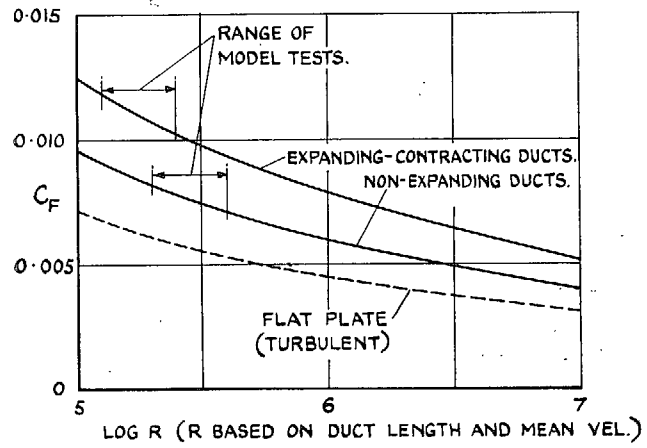

FIG. 18. Suggested variation of effective skin-friction coefficient with Reynolds number.

FIGS. 17 and 18. Duct loss.

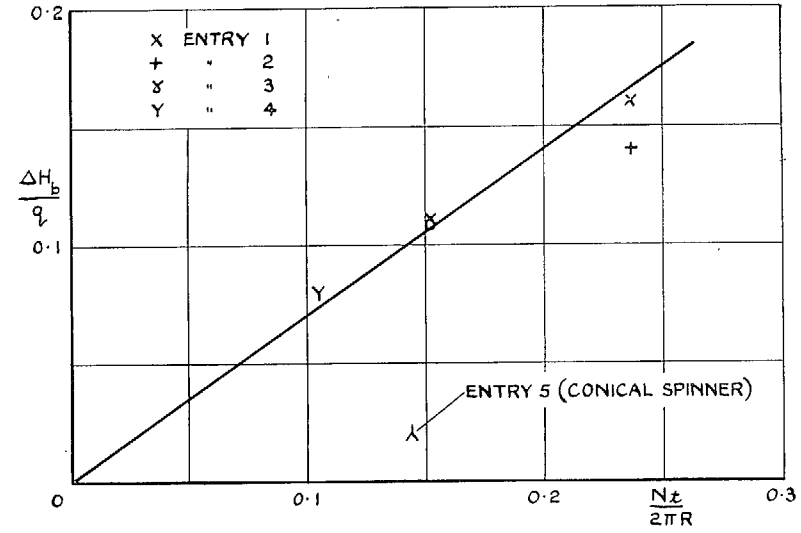

(a) MODEL RESULTS

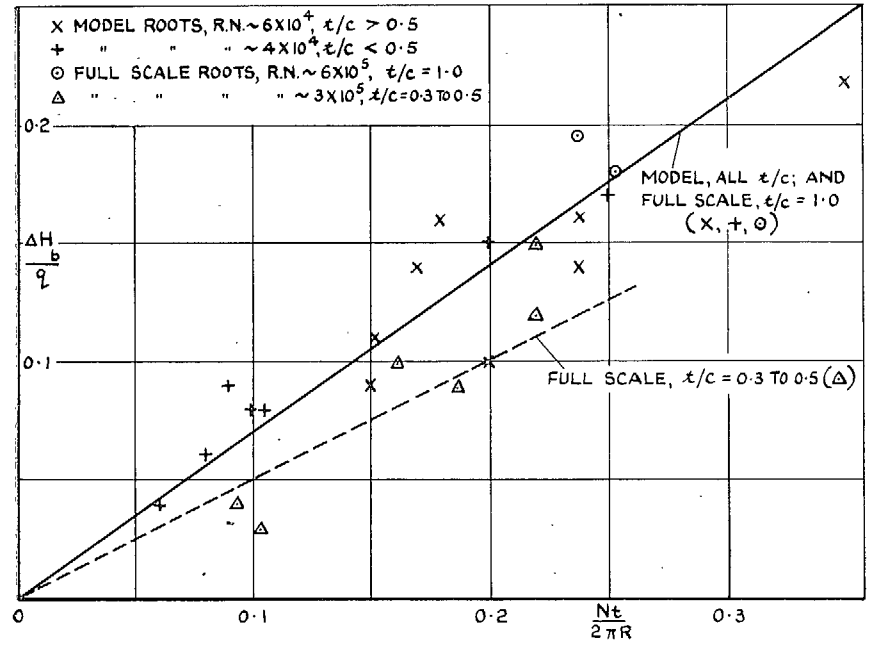

(b) COLLECTED MODEL AND FULL SCALE RESULTS.

FIG. 19. Blade-root loss.

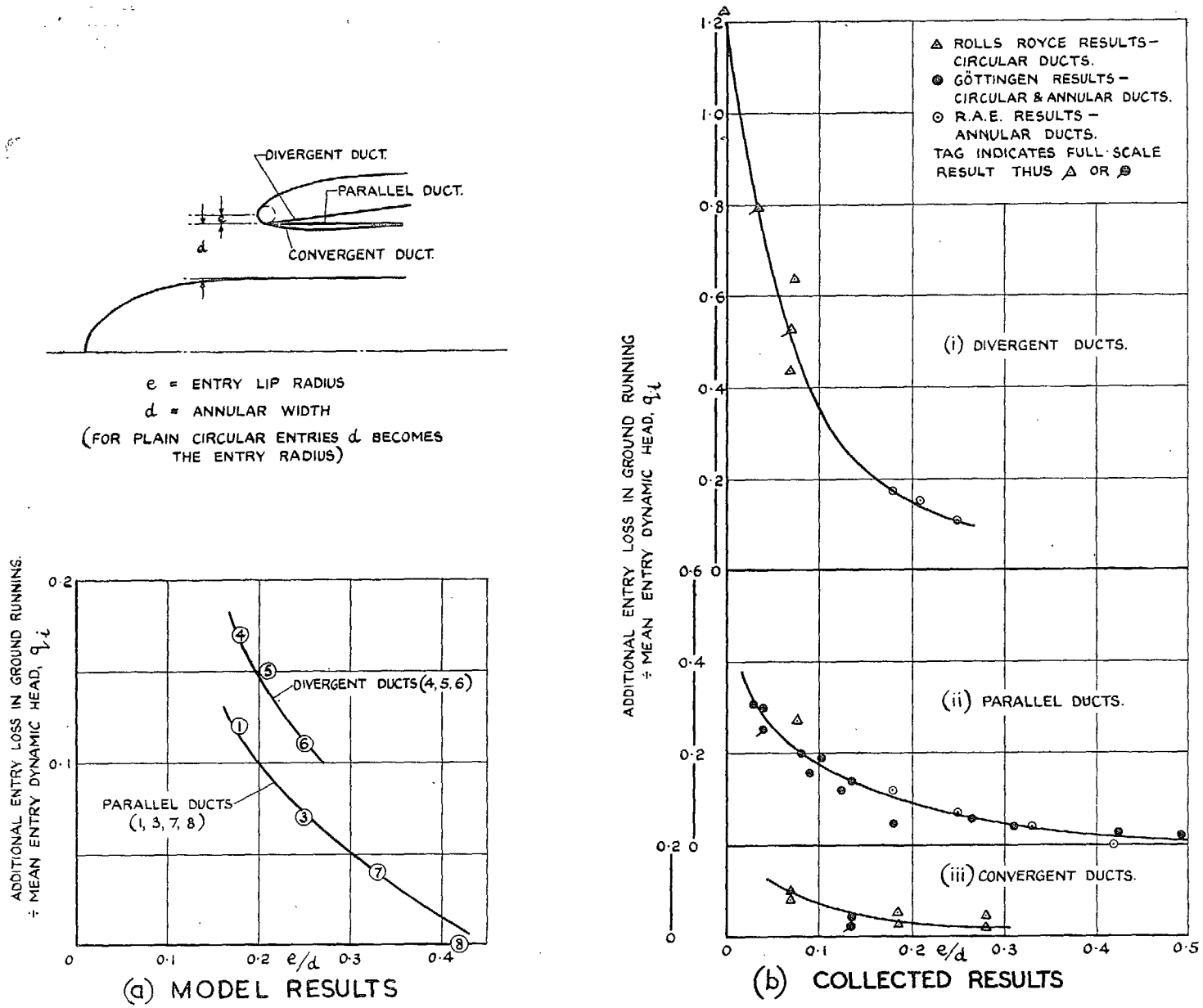

FIGS. 20a and 20b. Additional entry loss in ground running.

PART II

Ducted Spinners

1. *Introduction.*—A ducted spinner, in the present application, is primarily a device for reducing entry loss caused by the propeller blade roots by enclosing them in a low-velocity duct. The results of Part I showed that on a typical propeller-turbine layout with a conventional annular entry, the blade-root loss in high-speed or cruising flight may amount to 15 per cent of free-stream dynamic head*, out of a total entry loss of 25 per cent free-stream head. Coupled with this, electric tank experiments[2] determining the potential-flow pattern ahead of annular entries show that in most cases the velocity past the blade roots has practically the free-stream value. The problem of reducing blade-root loss is therefore virtually solved if the local velocity can be reduced to, say, one-third of flight speed. This figure is quite normal in ducted intake systems, hence follows the idea of a ducted spinner.

The general form of the layout, shown in Fig. 1, is already familiar. Ducted spinners have been tested previously, both here[3] and in America[4]; but in each case the principle involved was different from the present one. The American work, on NACA Cowl E for radial air-cooled piston engines, was concerned primarily with the development of a cowling having a high critical Mach number, and for this reason the entry area of the spinner was relatively small. On the other hand, the object of the tests described in Ref. 3 was to improve the cooling of piston engines on the ground; consequently the blade root fairings (*see* Fig. 1) were designed to give a high pressure rise. In neither case was the emphasis on providing a low-velocity duct to reduce internal loss.

The chief disadvantage associated with a ducted spinner is the increase in power plant weight, which must be set against any advantage obtained by way of increased thrust or lower specific fuel consumption, arising from reduction of the entry loss. It is however outside the scope of the present report to attempt to consider the balance of these factors. On the purely aerodynamic side, there are other obvious complications and possible disadvantages in the scheme. Thus the addition of casings round the blade roots increases the total root blockage. The existence of a clearance gap, or leak, between the rotating cowl and main nacelle means that more flow is taken through the spinner than is required for the engine. Both these factors will tend to increase the loss in the spinner itself. Other effects of the leak need careful attention; for example, assuming there is no change of duct area at the position of the leak, then loss of flow through the leak will create a pressure rise in the duct, which may affect the stability of the duct boundary layers. A further point is that, to get full benefit from the scheme, not only the spinner but the complete entry must be designed for low velocity; hence the rear duct will be different from that which would be used without the ducted spinner.

To obtain information on these and other points, and to check the efficiency of a ducted spinner entry in a practical case, the present experiments were undertaken. Model tests were made of a number of alternative designs for the Napier Naiad engine, and also of an annular entry of similar type to those tested in Part I. The results are compared and general conclusions are drawn. In a separate section of the report, a detailed analysis of the ducted spinner losses is made, which shows how methods evolved in Part I can be used for estimating losses in this type of entry also.

2. *Details of Model and Tests.*—The tests were made in the R.A.E. 5-ft Open-Jet Wind Tunnel, between September, 1946, and March, 1947. The model was generally similar to that used for annular entries in Part I. It consisted of a long cylindrical ducted nacelle, the front end representing the Naiad intake on $\frac{3}{8}$-scale. Interchangeable nose-pieces were supplied for the different cases. The general arrangement is shown in Fig. 2, and Fig. 3 is a photograph of the fully instrumented model mounted in the tunnel.

*Free-stream dynamic head is often termed ' ram '; which expression is occasionally used, for brevity, in the present report.

A single electric motor was housed inside the model to drive the spinner. The exit area at the rear of the nacelle could be varied by sliding the outer cowl over a tapered bullet, the last stage of opening being provided by an attachable conical gill-plate. This gave a low range sufficient to cover top speed, cruising, and climbing conditions. The range was, of course, considerably more restricted than that provided by internal fans on the Part I model[1] : in particular, it was not possible to represent ground running and take-off conditions.

Behind the spinner itself was a fixed rear duct, forming part of the complete entry. The terminology is illustrated in Fig. 1. Total head and static pressure were measured at the end of the rear duct, this corresponding to the compressor inlet of the engine. The measurements were made by means of eight 5-pitot combs spaced round the annulus (a total of 40 readings), eight static tappings on the outer wall and four on the inner. These readings were used to determine (*a*) the flow and velocity distribution, and (*b*) the mean total head and hence the entry loss. The flow out of the leak was measured by means of single pitot and static-tubes inserted in the gap, the line of the tubes being adjusted to the mean direction of flow, as observed by a wool tuft. The arrangement can be seen in Fig. 3. Owing to the presence of a high velocity gradient across the narrow gap, and to fluctuations in gap width as the spinner rotated, the accuracy of measurement of the leak flow was low. An average error of $\pm$ 15 per cent is estimated, which on total flow, however, amounts to only 3 per cent at the smallest flow and 2 per cent at the highest. The average error of the duct flow measurement is estimated to be much less than this.

Particulars of the various entries are listed below.

The following nomenclature is adopted :—

D	ducted spinner
L or S	long or short cowl
F or C	faired or circular blade-root casings
I	idealised rear duct (*see* (iv) below).

The entries are shown in Figs. 4 to 7.

(i) *D/L/F* (*Fig.* 4) : Ducted spinner with long outer cowl (entry right at the nose) and faired roots. The fairings were not of good aerodynamic shape, in that firstly, long fairings were required to support the outer cowl, so the maximum thickness, governed by the position of the propeller, was at about 60 per cent chord ; and secondly, the end of the fairing was cut off bluffly because of space restriction behind the propeller.

(ii) *D/L/C* (*Fig.* 4) : Ducted spinner with full-length outer cowl and circular cylindrical sleeves enclosing the blade roots. Support of the outer cowl was completed by four small streamlined struts (not shown in Fig. 4) running across the annulus near the entry. The purpose of this version was to check, by comparison with D/L/F, the importance of fairing the blade roots.

(iii) *D/S/F* (*Fig.* 5) : Ducted spinner, with shortened outer cowl and faired roots. This performs the main function of shrouding the blade roots, and has advantages over the long-cowled versions in being lighter in weight and allowing for better-shaped fairings. The projecting nose of this spinner makes the entry condition similar to that of an annular intake without propeller (Part I) ; and the entry area must be chosen so that the boundary-layer flow on the nose is stable up to the highest velocity ratio* to be used.

* Velocity ratio is V/V_i where V is free-stream velocity and V_i is mean entry velocity.

(iv) *D/L/F/I (Figs. 4 and 7)* : Spinner D/L/F used in conjunction with an ' idealised ' rear duct. In each of cases (i) to (iii), the rear duct was blocked at top and bottom by thick gear box fairings running the full length of the duct. Consequently the duct had a fairly small area and rapid changes of shape, as Figs. 4 and 7 show. Since this is a function of engine and auxiliary layouts, and only one of many possible arrangements, it was decided to separate its effect from the ducted spinner results by means of the present test, for which the blockages were removed entirely, leaving a completely annular duct of the same profile as before, but with considerably greater area.

(v) *Annular entry (Fig. 6)* : Similar to those tested in Part I, but directly comparable with ducted spinners (i) to (iii) ; including a similar blockage in the rear duct.

The ducted spinners each had four blade-root casings, corresponding to a 4-blade propeller. There were no blades outside the spinner. The annular entry was tested with a 4-blade model propeller, cropped to about half-diameter in the usual way for this type of test.

A curve showing the variation of net duct area from entry to compressor inlet is given with the drawing of each spinner. The ducted spinners had an entry area of 1·73 sq ft full-scale, compared with 1·17 sq ft for the annular entry, and in general a large area was maintained as far as possible down the duct. This was particularly so in the case of D/L/F/I. All the entries had of course the same area (0·52 sq ft) at the compressor inlet position. Within the ducted spinners themselves, no adjustment of area was made to allow for the blockage of the blade-root casings, since it was thought doubtful whether changing the profile of the duct locally to compensate would be profitable. The results have some bearing on this point (*see* section 5).

For spinners D/L/F and D/S/F, the blade-root casings were set at a mean angle of 54 deg from no-lift to the plane of propeller rotation, the no-lift angle of the D/L/F casings being judged from results for similarly shaped fairings in Ref. 3. Apart from any effect of boundary layers on the inside surfaces of the spinner ahead of the roots, the fairings were at zero lift for $\lambda = V_d/\pi nD = \tan^{-1} 54 \text{ deg} = 1 \cdot 4$*. This value corresponded to estimated cruising r.p.m. and air flow.

The measurements with each entry were made over a range of spinner speeds at each value of the flow. For the most part the model was at 0 deg incidence, but additional tests at 6 deg and 12 deg were made in the case of spinner D/S/F, and with the annular entry. A wind speed of 120 ft/sec was used, with occasional tests at 80 and 180 ft/sec to check scale effect. Tests of the annular entry were made at two blade angles and also without propeller.

3. *Results.*—3.1. *General.*—Results of the measurements are given in full in Tables 2 to 6 and plotted in Figs. 9 to 16. Figs. 9, 11, 13 and 15 show entry total head plotted against flow for each of the spinners. The flow is represented by the inverse velocity ratio V/V_c (V being the free-stream velocity and V_c the mean velocity at the compressor inlet, where all arrangements have the same area) following the method used in Part I ; and the scale is best regarded as one of flight speed for a given engine flow. The full curves give the results at constant spinner r.p.m.; and a few curves for constant $\lambda (= V_d/\pi nD)$ have been dotted in. For any flight condition (defined by the values of V/V_c and λ) within the range covered by the tests, the total head, or ' percentage ram recovery,' can immediately be seen.

In the alternate diagrams (Figs. 10, 12, 14 and 16) results are plotted in the form of fan characteristics, as used for example in Ref. 3. In these the total-head rise through the spinner (measured from free stream to compressor inlet, and normally negative in the present tests) is expressed in terms of the mean rotational head $\frac{1}{2}\rho(\pi nD)^2$, and plotted against λ. This gives a useful check on the accuracy of the measurements, because so long as the net loss is made up of a pressure rise (or drop) from the fan action of the blade-root casings, and a duct loss which is proportional

---

* V_d axial velocity of flow, based on annular area neglecting blockage of roots
n spinner rotational speed
D mean diameter of annulus.

to the square of duct velocity and hence in the present form simply a constant times λ^2, a single curve is obtained for all spinner r.p.m. and exit settings. When, however, an additional loss dependent on external conditions occurs, curves for different values of V/V_c separate out. This happens in two cases, those of spinners D/S/F (Fig. 13) and D/L/F/I (Fig. 16) ; and thereby reveals certain interesting results, which are discussed in later sections.

We are concerned mainly with examining and comparing results for $\lambda = 1{\cdot}4$, corresponding to zero lift on the faired root casings. Figs. 17 and 18 are prepared for this purpose. Fig. 17 shows the curve of total head against velocity ratio for each ducted spinner at $\lambda = 1{\cdot}4$, and also a comparable curve for the annular entry taken from the results in Table 6. Loss coefficients are given in Fig. 18 in the usual analytical form, in which the total entry loss is expressed in terms of mean entry dynamic head, q_i, and plotted against velocity ratio at entry, V/V_i. In this case the coefficients are directly comparable in magnitude, since all the spinners have the same entry area.

Fig. 19 shows the relation between V/V_i and V/V_c. This is not a simple area ratio because the entry velocity V_i includes the leak flow, while the compressor velocity V_c does not. The ratio of total flow through the spinner (rear duct flow + leak flow) to flow through the rear duct is plotted in the same diagram.

3.2. *Comparison with Annular Entry.*—Fig. 17 shows clearly the large improvement in intake efficiency which is possible with ducted spinners. For example, at $V/V_c = 1{\cdot}3$ each of the ducted spinners gives about 90 per cent total head at the compressor, compared with 72 per cent for the annular entry. Assuming the velocity at the compressor inlet to be 400 ft/sec, this velocity ratio would correspond to a flight speed of 350 m.p.h., and the advantage of 18 per cent ram would be equivalent to about 5 per cent increase of engine thrust or 3 per cent decrease in specific fuel consumption.

With the long cowled spinners D/L/F and D/L/C the advantage is still greater at higher velocity ratios, *i.e.*, higher flight speeds for a given engine flow. This is because, in the absence of external boundary layers, there is no real upper limit to the velocity ratio for which the nose entry can be designed, and therefore, since the duct velocity is a decreasing proportion of flight speed as the latter is increased, the percentage total head goes on increasing indefinitely.

In all cases the gain falls off at lower velocity ratios. Broadly this is because whereas with an annular entry the largest loss component is the blade-root loss, which is roughly a constant fraction of free-stream dynamic head (*see* Ref. 1), with a ducted spinner the largest component is internal duct loss, which is independent of forward speed and therefore, expressed as percentage q, increases as q decreases. The advantage could be partly restored by increasing the area through the spinner and in the first part of the rear, so that the duct loss for a given compressor velocity is reduced ; and this should be fully considered when designing a ducted spinner specially for lower flight speeds. On a normal power plant the practical limitation is set by the necessity for maintaining a reasonable outside shape, but in some cases an installed unit might have space available for a useful enlargement of the duct. From this point of view it is also profitable to restrict the leak flow to a minimum, so as to keep the velocity ratio in the spinner as high as possible.

3.3. *Faired or Circular Roots.*—Fig. 17 shows that while there is undoubtedly an advantage in fairing the blade-root casings, as in spinners D/L/F and D/S/F, the practical gain compared with the circular sleeves of spinner D/L/C is small (only 1 per cent q at 350 m.p.h.). This is to be expected, since at 350 m.p.h. ($V/V_c = 1{\cdot}3$) the velocity over the roots is only one-third of flight speed, so that the total loss caused by circular sleeves having a drag coefficient of $1{\cdot}0$ and a blockage ratio* of $0{\cdot}3$ would be less than 3 per cent q. There is little to choose between the differently shaped fairings of D/L/F and D/S/F, the advantage at low velocity ratio (where the entry conditions are equally good) being, as expected, with D/S/F.

* *i.e.*, (total frontal area of sleeves) + (total annular area of duct).

Insensitivity of the results to the shape of the blade-root casings emphasises the value of low internal velocity, which, as has been said, is the fundamental principle of the scheme.

3.4. *Long or Short Cowl.*—Results for the long and short cowl spinners, D/L/F and D/S/F, are not greatly different in the practical range of velocity ratio for which they were designed; but at high V/V_c, the efficiency of D/S/F falls off, owing to flow separation from the projecting nose of the spinner, caused by the adverse pressure gradient accompanying a high velocity ratio at entry. The effect is similar to that which occurs (to a greater degree) with annular entries[1]. It is shown in Fig. 18 by a rise in loss coefficient, and in the fan characteristic (Fig. 13) by a separation of points at the highest velocity ratio from the main curve. From Fig. 18 the limiting velocity ratio for stable flow on the nose is about $V/V_i = 4$ (corresponding $V/V_c = 1{\cdot}4$): this value conforms to the generalised curve deduced from Part I experiments (Fig. 15 or Ref. 1).

In practice, owing to its lower weight, spinner D/S/F would be preferable for all conditions up to a V/V_c of at least $1{\cdot}5$, *i.e.*, a flight speed of 400 m.p.h. for a compressor velocity of 400 ft/sec. At higher flight speeds the long cowl version might show a worthwhile advantage.

3.5. *Rear Duct Blockage.*—The 90 per cent ram given by the ducted spinners in level flight conditions ($V/V_c = 1{\cdot}3$) would be considerably higher but for the effect of the gear-box fairings in the rear duct, which, in the arrangement tested, greatly restrict the available duct area and have themselves an appreciable form drag. The final curve in Fig. 17 gives the result for entry D/L/F/I, *i.e.*, spinner D/L/F with a rear duct containing no blockage. We see that up to $V/V_c = 1{\cdot}3$) the loss is only half that of the other arrangements. In other words, under favourable conditions a ducted spinner entry can be expected to give about 95 per cent ram in level flight. This still makes no allowance for scale effect, which would be small but favourable (*see* section 4).

Apart from its effect on mean total head, the rear duct blockage upsets the flow distribution at the compressor. A typical result is shown in Fig. 8 where the velocity directly behind the struts is as much as 35 per cent below the mean. Such a variation may reduce appreciably the compressor efficiency, and may also lead to mechanical difficulties, arising from rapidly fluctuating loads on the rotor blades of the first stage.

It is therefore important to keep the rear duct blockage to a minimum, and if possible distributed so that individual fairings are not more than say 30 per cent thick. Failing this, a rapid contraction of the duct over the rear part of the fairings would improve the distribution, possibly at the expense of slightly lower mean total head. These conclusions apply equally to annular entries as to ducted spinners.

3.6. *Effect of Leak on Rear Duct Loss.*—One general effect associated with the leak which has not received attention in previous investigations is as follows. The outflow from the leak is accompanied by a decrease in velocity, and a consequent rise in pressure, in the duct*. This pressure rise may affect the stability of the boundary layer on the opposite wall of the duct, and in some circumstances cause a separation. With a given entry, the effect will be most marked at the highest velocity ratio, where the proportion of leak flow to total flow is greatest. The results for spinners D/L/F and D/L/C, in the form presented in Figs. 10 and 12, show no evidence of loss increasing with increase of velocity ratio. Spinner D/S/F (Fig. 14) does show such an effect but the explanation (section 3.4) is in this case different. In all three cases, the leak is followed by a contraction in the rear duct, as shown in the area curves of Figs. 4 and 5. It may be inferred that any tendency to separation is suppressed by this contraction. But in the case of spinner D/L/F/I, owing to removal of the rear struts, the duct has an expanding region immediately behind the leak (Fig. 4), which must increase the tendency to separation. The results in Fig. 16 indicate that separation actually occurs above a velocity ratio (V/V_c) of about $0{\cdot}9$, *i.e.*, when the

* This assumes no change in duct area across the leak. If the duct area were changed, *e.g.*, by having a forward-facing entry for the leak flow, the compensation would only be exact at one particular velocity ratio, *i.e.*, in general for one particular flight condition.

leak flow (Fig. 19) is more than about 10 per cent of the total. This causes the total-head curve in Fig. 17 to flatten off at high velocity ratio, and accounts for the rising loss coefficient shown in Fig. 18.

It is concluded that (*a*) the leak flow should be minimised by restricting the gap—this has already (section 3.2) been shown to be desirable from another aspect—and (*b*) while taking advantage of every possibility for maintaining a large duct area, actual expansion of the duct in the neighbourhood of the leak should be avoided.

3.7. *Effect of Incidence.*—The effect of inclination of the nacelle on total head at the compressor is small. Measurements at 6 deg and 12 deg incidence are included in Tables 4 and 6. With spinner D/S/F at low velocity ratio, the mean total head decreases at the rate of 1 per cent q per 4 deg incidence. With long cowl spinners the decrease would be slower. For the annular entry, on the other hand, the rate is 1 per cent q per 2 deg : this is the same result as was obtained in Part I.

4. *Analysis of Losses.*—The total loss in the various ducted spinner entries can be regarded as made up of the following components :—

(*a*) Duct friction loss. This can be subdivided futher into two parts, that occurring in the spinner itself and that in the rear duct

(*b*) Blade-root loss. By this is meant the loss arising from the form drag of the blade-root casings

(*c*) Spinner loss. Applies to D/S/F only and refers to boundary-layer development on the projecting nose of the short-cowl spinner. Corresponds to the total spinner loss of an annular entry[1], for which reason the same terminology is used

(*d*) Rear strut loss. Applies to all except D/L/F/I, and refers to loss caused by form drag of the gear box fairings in the rear duct

(*e*) Rear duct separation loss. The effect of the leak, discussed in section 3.6. Applies to D/L/F/I only.

Only the total loss was measured, but by comparing suitable cases and using generalised results from Part I, a fairly accurate quantitative analysis can be made. Details of the method are given in an Appendix. Results of the analysis are shown in Figs. 20 to 23, in which the total loss for each spinner ($\lambda = 1{\cdot}4$) and the component losses are plotted against velocity ratio. It is seen that in all cases except that of D/L/C, the blade-root drag is less than 2 per cent free-stream dynamic head. Thus the first objective of the ducted spinner entry has been achieved. In the three practical cases, rear strut loss is excessive by comparison with the rest. Rear strut loss is a function of the engine layout, and virtually independent of whether a ducted spinner is used or not. The result for D/L/F/I shows what might be possible in a favourable case. Even this is not ideal, owing to the rear duct separation loss, which could be prevented by altering the shape of the duct. The analysis for D/S/F shows the crucial range of velocity ratio, above which spinner loss becomes excessive. In this case the form drag of the blade-root fairings is negligibly small.

A detailed comparison with the annular entry at $V/V_c = 1{\cdot}3$ (flight speed 350 m.p.h. for a compressor inlet velocity of 400 ft/sec) is made in the following table. The annular entry loss has been analysed on lines similar to the above, though in this case there is evidence of interaction between blade-root loss and rear strut loss which makes the analysis more doubtful. The conclusions of Part I on blade-root loss have been used, however, as a check.

Comparison of Ducted Spinners with Annular Entry ($V/V_c = 1{\cdot}3$)

Entry	Total measured loss ÷ q	Loss analysis					Full-scale estimate	
		Duct (total)	Blade roots	Spinner nose	Rear struts	Rear duct separation	Total loss ÷ q	per cent ram recovery
D/L/F	0·095	0·04	0·015	—	0·04	—	0·08	92
D/L/C	0·105	0·035	0·03	—	0·04	—	0·09	91
D/S/F	0·105	0·035	0	0·03	0·04	—	0·09	91
D/L/F/I	0·055	0·025	0·015	—	—	0·015	0·04	96
Annular	0·28	0·035	0·17	0·04	0·035	—	0·25	75

The dominant feature of the comparison is the large reduction in blade-root loss achieved by the ducted spinners.

In the last two columns an estimate for full-scale entries is given, in which allowance has been made for scale effect on the friction components of the loss. Scale effect on the rear strut drag is unpredictable : it might reduce the losses by a further two or three per cent q, without affecting differences between the various cases.

5. *Concluding Remarks.*—The tests have shown that a ducted spinner entry will give 90 to 95 per cent ram recovery in normal cruising flight. Where the alternative annular entry, behind the propeller roots, would give only 70 to 75 per cent ram* (which is the case with most of the arrangements tested in Part I), this represents a considerable improvement, which could be expected to show a net gain when offset against the increase in power plant weight. The essential feature of the scheme is to provide a low velocity of flow past the blade roots. In terms of the parameter used in the report, this means that the velocity ratio V/V_i must be as high as possible ; *i.e.*, the bigger the duct or the higher the flight speed (or both), the greater is the advantage of the ducted spinner. With a full-length outer cowl, extending to the nose of the spinner, the increase in ram with increase of V/V_i, at small incidences, continues indefinitely, though above $V/V_i = 4$ improvement is small.

The weight and structural problems can be eased by shortening the outer cowl so that it just covers the fairings round the blade roots. In this case the percentage ram begins to fall off around $V/V_i = 4$, but the value is normally sufficient to give a ram recovery of about 95 per cent.

The blade-root loss having been greatly reduced in this way, duct loss becomes the major component. It is therefore important that the high velocity ratio in the spinner should be maintained as far as possible down the duct, by keeping the area large. An annular entry has to work at a lower velocity ratio (*see* Ref. 1), and it follows that only partial improvement will be obtained if the ducted spinner is matched up to a rear duct which has been designed as an annular entry. The only qualification to this is that care must be taken to avoid expanding the duct in the immediate neighbourhood of the leak (*see* section 3.6).

Since the whole blade-root loss in a ducted spinner is only of the order of 2 to 4 per cent q, it follows that changes arising from differently shaped root fairings are small. The same can be said of moderate changes in duct shape, such as would be involved, for example, in compensating the duct area for blockage of the root fairings. Nevertheless the tests show that ordinary aerodynamic considerations do apply, and the total gain possible by observing the usual principles of good shape within the spinner and duct is not negligible.

* The statement is put in this way because propeller roots do vary a good deal, and since they contribute the major part of the loss with an annular entry, considerable variation from the 70 to 75 per cent figure is possible in certain cases. A proper estimate for the annular entry should always be made, using the generalised results in Ref. 1.

Ground running characteristics have not been measured directly in the present tests. To avoid additional loss at entry in this condition, the general principles laid down in Part I (section 4.4) should be observed ; *e.g.*, the nose radius of the outer cowl should be of the order of 0·1 times the annular entry width. Providing this is done the flow in the spinner will be practically independent of forward speed, so that results for ground running can be estimated from the fan characteristic curves in Figs. 10, 12, 14 and 16. The axial velocity in the spinner will tend to be smaller than in cruising flight, because of the higher density at ground level, and also because at very low forward speed the flow through the leak is inwards, so the spinner now takes less flow than is required by the engine. This means that the appropriate value of λ will be lower than 1·4. In general the tests include values of down to 0·7 which is sufficient to cover the ground running case.

Acknowledgments.—The authors wish to acknowledge the share of work done by J. Kinsella and A. H. Stratford, members of the staff of Napier Ltd., who assisted throughout the tunnel tests and did most of the working out of results. Thanks are due to Messrs. Napier for their help and full co-operation in this arrangement. D. J. Kettle, of the R.A.E., also assisted.

LIST OF SYMBOLS

ρ		Density of air
V		Free-stream velocity
q		Free-stream dynamic head $= \frac{1}{2}\rho V^2$
V_i		Mean velocity at entry
V_d		Mean velocity in spinner at propeller centre-line position
V_c		Mean velocity at compressor inlet
q_c		Dynamic head at compressor inlet $= \frac{1}{2}\rho V_c^2$
D		Mean internal diameter at propeller centre-line position
n		Rotational speed of spinner
λ	$=$	$V_d/\pi nD$
H_c		Mean total head at compressor inlet
ΔH		Loss of total head up to compressor inlet $= q - H_c$
ΔH_d		Loss of total head from friction in duct
A		Cross-sectional area of duct
A_c		Cross-sectional area at compressor inlet
r_O		Outer radius of annulus
r_I		Inner radius of annulus
x		Axial distance along duct
C_F		Effective skin-friction coefficient of duct
I		Geometric integral for whole or part of duct $= 2\int\left(\frac{A_c}{A}\right)^2 \frac{dx}{(r_O - r_I)}$
D/L/F		Ducted spinner with long cowl and faired root casings
D/L/C		Ducted spinner with long cowl and circular root casings
D/S/F		Ducted spinner with short cowl and faired root casings
D/L/F/I		Ducted spinner with long cowl, faired root casings, and idealised rear duct

REFERENCES

No.	Author	Title, etc.
1	J. Seddon and A. Spence	A wind-tunnel investigation of entry loss on propeller-turbine installations. Part I: Annular entries behind propeller. Part I of this Report. A.R.C. 11,602. March, 1948.
2	H. Hahnemann and K. Bammert ..	Electric tank tests of propeller-turbine intakes. M.A.P. Völkenrode unpublished reports, 1946.
3	J. Seddon, M. F. Mullins and D. J. Harper	Wind-tunnel model tests on the cooling and drag characteristics of two hollow spinner fans, suitable for a radial air-cooled engine or annular ring radiator mounted behind a tractor propeller. R.A.E. Report Aero. 2085. October, 1945.
4	J. G. McHugh	Progress report on cowlings for air-cooled engines investigated in the N.A.C.A. 19-ft Pressure Wind Tunnel. N.A.C.A. Advance Restricted Report. A.R.C. 5333. July, 1941.

APPENDIX

Method of Analysing Ducted Spinner Loss

(*a*) Duct loss for each entry is estimated by means of the relation

$$\frac{\Delta H_d}{q_c} = C_F I = 2C_F \int \left(\frac{A_c}{A}\right)^2 \frac{dx}{(r_O - r_I)} ,$$

derived in Part I.

$\Delta H_d/q_c$ duct loss referred to dynamic head at compressor inlet ;

A_c/A duct area at compressor inlet ÷ area at x ;

r_O, r_I outer and inner radii of annulus at x ;

x axial distance along duct ;

C_F effective skin-friction coefficient, whose value is taken to be 30 per cent above that for a flat plate in turbulent flow at the same Reynolds number. The integral is taken along the whole or part of the duct as required.

(*b*) From the fan characteristic curves for spinner D/L/F/I (Fig. 16) the rear duct separation loss is obtained as a function of velocity ratio.

(*c*) Adding this to the duct loss, the residue from total measured loss of D/L/F/I is attributed to form drag of the blade-root fairings. The same blade-root loss is then assumed for spinner D/L/F.

(*d*) The excess loss of D/L/F over D/L/F/I, after allowing for the difference in duct loss and for rear duct separation loss in the latter, represents form drag of the rear struts. This is applied also to spinners D/L/C and D/S/F.

(*e*) Blade-root loss for D/L/C is now obtained by difference from total measured loss.

(*f*) The residual loss of D/S/F is made up of spinner loss and blade-root loss. Using generalised results for spinner loss from Part I, it is deduced that this accounts for the whole residue, *i.e.*, the form drag of the blade-root fairings is in this case negligibly small.

TABLE 1

Model Data (Dimensions given Full-Scale)

Scale		$\frac{3}{8}$
Ducted spinners :—		
Entry area, A_i		1·73 sq ft
Area at propeller centre-line*		1·60 „ „
Area at compressor inlet, A_c		0·52 „ „
Mean internal diameter at propeller centre-line, D		1·615 ft
Leak exit areas :—	D/L/F	0·16 sq ft
	D/L/C	0·19 „ „
	D/S/F	0·12 „ „
	D/L/F/I	0·17 „ „
Number of blade-root fairings		4
Annular entry :—		
Entry area, A_i		1·17 sq ft
Area at compressor inlet, A_c		0·52 sq ft
Diameter of cropped propeller		3·33 ft
Number of blades		4
Assumed level flight conditions :—		
Forward speed, V		350 m.p.h.
Air consumption		210 cu ft/sec
Compressor inlet velocity, V_c		400 ft/sec
Velocity ratio V/V_c		1·3
Leak flow ÷ engine flow		0·15
Propeller r.p.m.		1250
λ ($= V_a/\pi nD$) for ducted spinners		1·4

* Ignores blockage of blade roots.

TABLE 2

Results for Spinner D/L/F

$\alpha = 0$ deg; Tunnel speed = 120 ft/sec

Exit No.	r.p.m.	Flow		λ	$\frac{H_e}{q}$	Total-head loss	
		V/V_i	V/V_e			$\div q$	$\div \frac{1}{2}\rho(\pi nD)^2$
1	2400	2·07	0·658	0·82	0·903	0·097	0·24
	1800	2·16	0·686	1·05	0·759	0·241	1·06
	1400	2·22	0·707	1·32	0·702	0·298	2·18
2	2400	2·36	0·781	0·72	1·011	−0·011	−0·03
	1800	2·51	0·826	0·91	0·901	0·099	0·44
	1400	2·55	0·848	1·14	0·816	0·184	1·34
	1000	2·61	0·863	1·57	0·785	0·215	3·09
	750	2·64	0·870	2·07	0·770	0·230	5·84
3	2400	2·62	0·920	0·65	1·071	−0·071	−0·18
	1800	2·79	0·974	0·81	0·972	0·028	0·12
	1400	2·88	1·000	1·01	0·901	0·099	0·72
	1000	2·96	1·017	1·38	0·853	0·147	2·11
	750	3·00	1·024	1·82	0·835	0·165	4·20
4	1400	3·22	1·146	0·91	0·948	0·052	0·37
	1000	3·29	1·168	1·24	0·895	0·105	1·50
	750	3·32	1·176	1·64	0·870	0·130	3·31

TABLE 3

Results for Spinner D/L/C

$\alpha = 0$ deg; Tunnel speed = 120 ft/sec

Exit No.	r.p.m.	Flow		λ	$\frac{H_e}{q}$	Total-head loss	
		V/V_i	V/V_e			$\div q$	$\div \frac{1}{2}\rho(\pi nD)^2$
1	2400	2·26	0·722	0·74	0·669	0·331	0·79
	1800	2·25	0·716	1·00	0·648	0·352	1·50
	1400	2·24	0·714	1·29	0·677	0·323	2·29
2	2400	2·63	0·867	0·64	0·761	0·239	0·57
	1800	2·64	0·874	0·85	0·750	0·250	1·07
	1400	2·62	0·867	1·10	0·757	0·243	1·72
	1000	2·62	0·864	1·54	0·779	0·221	3·08
3	1800	3·02	1·029	0·74	0·828	0·172	0·74
	1400	3·03	1·030	0·95	0·810	0·190	1·34
	1000	3·00	1·020	1·34	0·838	0·162	2·25
	750	3·00	1·017	1·79	0·844	0·156	3·86
4	1400	3·40	1·189	0·85	0·853	0·147	1·04
	1000	3·36	1·170	1·20	0·875	0·125	1·74
	750	3·35	1·168	1·60	0·879	0·121	2·99
5	1400	4·36	1·605	0·66	0·922	0·078	0·55
	1000	4·43	1·634	0·91	0·915	0·085	1·18
	750	4·37	1·613	1·23	0·928	0·072	1·78
	500	4·41	1·623	1·83	0·926	0·074	4·12

TABLE 4

Results for Spinner D/S/F

Exit No.	r.p.m.	Flow		λ	$\frac{H_e}{q}$	Total-head loss	
		V/V_i	V/V_e			$\div q$	$\div \frac{1}{2}\rho(\pi nD)^2$
$\alpha = 0$ deg : Tunnel speed = 120 ft/sec							
1	2400	2·10	0·663	0·80	0·783	0·217	0·52
	1800	2·16	0·689	1·03	0·745	0·255	1·10
	1400	2·21	0·699	1·30	0·724	0·276	1·95
2	2400	2·47	04801	0·68	0·891	0·109	0·26
	1800	2·58	0·834	0·87	0·838	0·162	0·69
	1400	2·64	0·852	1·09	0·815	0·185	1·31
	1000	2·66	0·858	1·52	0·792	0·208	2·90
3	1800	2·95	0·977	0·76	0·899	0·101	0·43
	1400	2·99	0·990	0·96	0·873	0·127	0·90
	1000	3·03	1·004	1·33	0·850	0·150	2·09
	750	3·06	1·009	1·76	0·834	0·166	4·09
4	1400	3·40	1·149	0·85	0·906	0·094	0·66
	1000	3·41	1·158	1·18	0·883	0·117	1·62
	750	3·45	1·168	1·56	0·869	0·131	3·24
5	1400	4·53	1·620	0·64	0·942	0·058	0·41
	1000	4·63	1·640	0·87	0·910	0·090	1·26
	750	4·65	1·658	1·15	0·897	0·103	2·54
	500	4·70	1·660	1·71	0·888	0·112	6·22
$\alpha = 6$ deg : Tunnel speed = 120 ft/sec							
1	2400	2·14	0·672	0·78	0·782		
	1800	2·17	0·689	1·03	0·740		
	1400	2·21	0·699	1·30	0·717		
$\alpha = 12$ deg : Tunnel speed = 120 ft/sec							
1	2400	2·15	0·677	0·78	0·762		
	1800	2·19	0·690	1·02	0·710		
	1400	2·23	0·700	1·29	0·691		

TABLE 5

Results for Spinner D/L/F/I

$\alpha = 0$ deg; Tunnel speed = 120 ft/sec

Exit No.	r.p.m.	Flow		λ	$\frac{H_e}{q}$	Total-head loss	
		V/V_i	V/V_e			$\div q$	$\div \frac{1}{2}\rho(\pi nD)^2$
1	1500	1·93	0·621	1·42	0·875	0·125	0·77
	1250	1·93	0·617	1·69	0·800	0·200	1·77
	1000	1·99	0·639	2·05	0·774	0·226	3·15
2	1500	2·27	0·758	1·19	0·961	0·039	0·24
	1250	2·29	0·762	1·42	0·911	0·089	0·79
	1000	2·32	0·770	1·76	0·854	0·146	2·04
	750	2·40	0·799	2·25	0·824	0·176	4·35
3	1500	2·64	0·914	1·02	1·002	−0·002	−0·01
	1250	2·67	0·922	1·21	0·958	0·042	0·37
	1000	2·71	0·928	1·50	0·920	0·080	1·11
	750	2·78	0·951	1·94	0·876	0·124	3·06
4	1250	3·09	1·096	1·04	0·985	0·015	0·13
	1000	3·12	1·109	1·29	0·947	0·053	0·74
	750	3·21	1·129	1·68	0·907	0·093	2·29
	500	3·32	1·168	2·43	0·869	0·131	7·30
5	1000	3·79	1·406	1·06	0·985	0·015	0·21
	750	3·88	1·445	1·40	0·948	0·052	1·28
	500	3·98	1·477	2·05	0·912	0·088	4·89
6	1000	5·48	2·336	0·74	1·007	−0·007	−0·10
	750	5·57	2·358	0·96	0·977	0·023	0·57
	500	6·00	2·625	1·35	0·946	0·054	3·00

TABLE 6

Results for Annular Entry

Tunnel speed = 120 ft/sec

Exit No.	r.p.m.	Flow V/V_i	Flow V/V_e	λ	$\frac{H_e}{q}$	$\frac{\text{Loss}}{q}$
$\alpha = 0$ deg : Blade setting for cruise						
1	1800	1·65	0·729	0·93	0·655	0·345
	1000	1·68	0·741	1·66	0·637	0·363
2	1800	2·07	0·919	0·74	0·687	0·313
	1000	2·06	0·912	1·34	0·687	0·313
3	1400	2·44	1·080	0·81	0·710	0·290
	750	2·43	1·078	1·52	0·712	0·288
4	1400	2·85	1·259	0·70	0·712	0·288
	1000	2·84	1·255	0·98	0·722	0·278
	750	2·84	1·253	1·30	0·721	0·279
$\alpha = 6$ deg : Blade setting for cruise						
1	1800	1·67	0·740	0·92	0·627	0·373
	1000	1·72	0·763	1·61	0·621	0·379
$\alpha = 12$ deg : Blade setting for cruise						
1	1800	1·66	0·734	0·93	0·608	0·392
	1000	1·74	0·771	1·59	0·588	0·412
$\alpha = 0$ deg : Blade setting for climb						
1	1800	1·69	0·748	0·91	0·633	0·367
2	1800	2·06	0·916	0·74	0·679	0·321
$\alpha = 0$ deg : No propeller						
1	~250	1·57	0·695	—	0·797	0·203
2	250	1·95	0·861	—	0·790	0·210
3	250	2·36	1·045	—	0·789	0·211
4	250	2·72	1·203	—	0·797	0·203

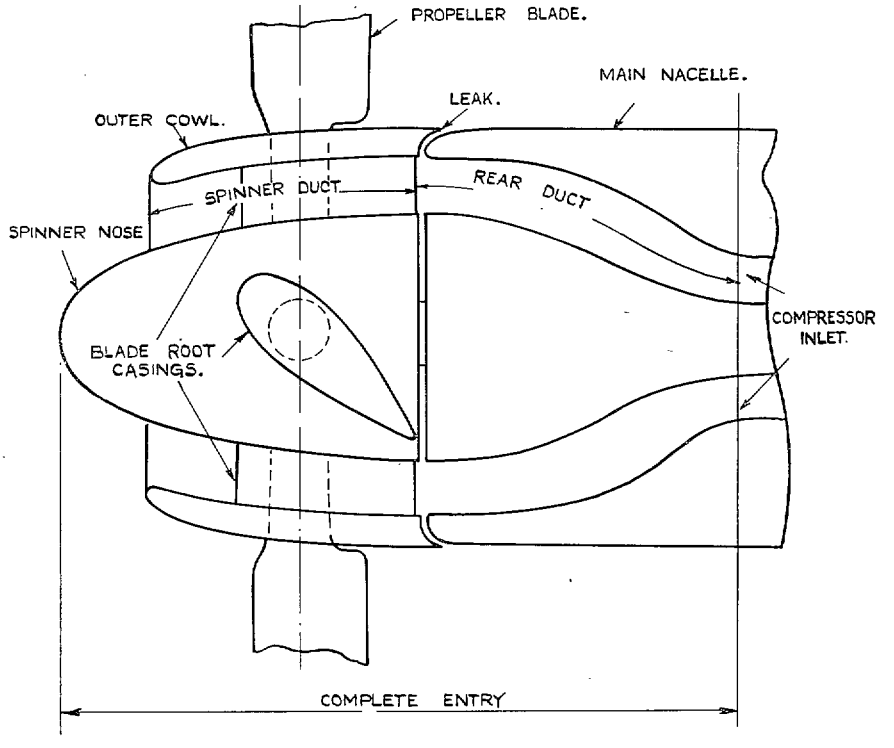

FIG. 1. Typical ducted spinner entry with terminology used in report.

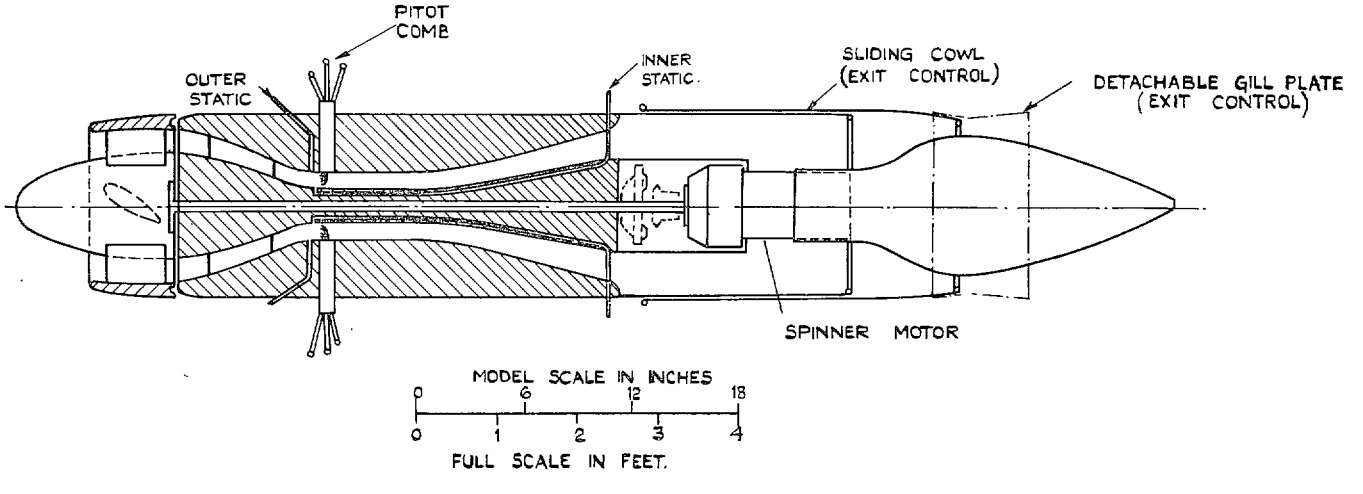

FIG. 2. General arrangement of model nacelle.

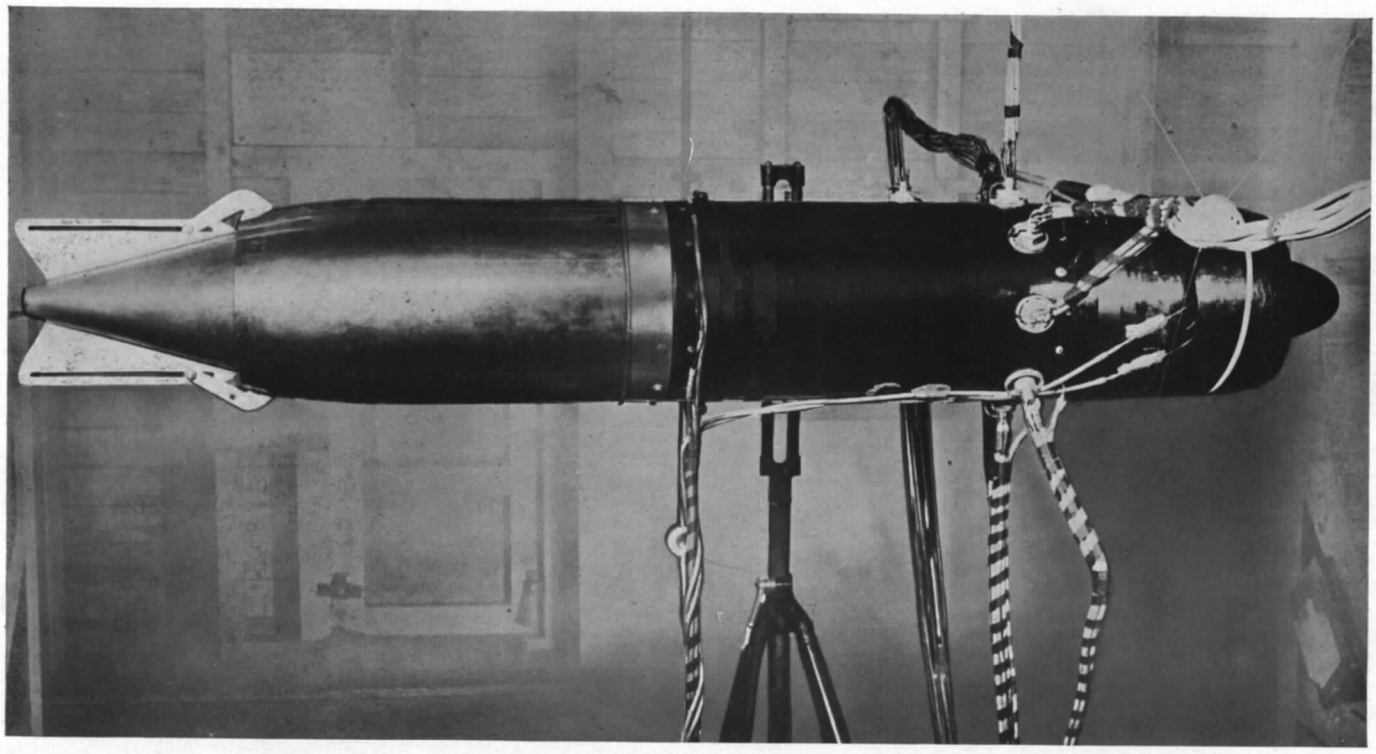

FIG. 3. Model nacelle in 5-ft Wind Tunnel.

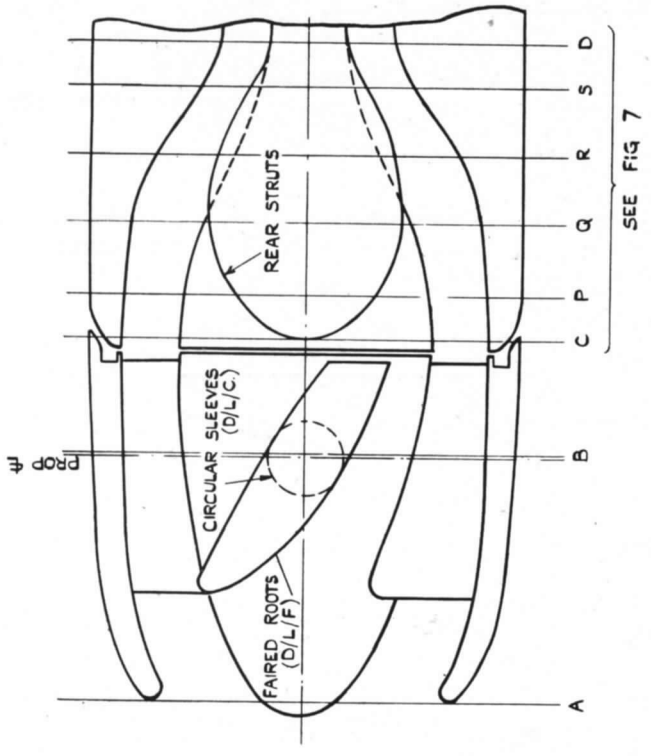

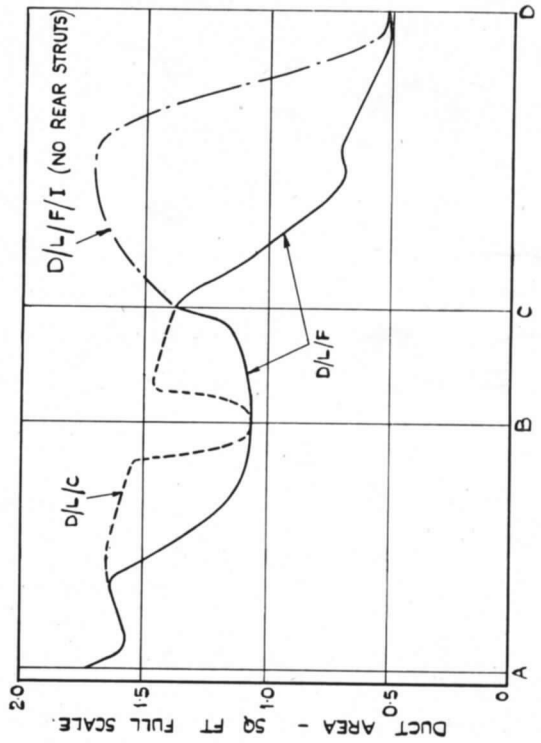

FIG. 4. Ducted spinners D/L/F, D/L/C and D/L/F/I.

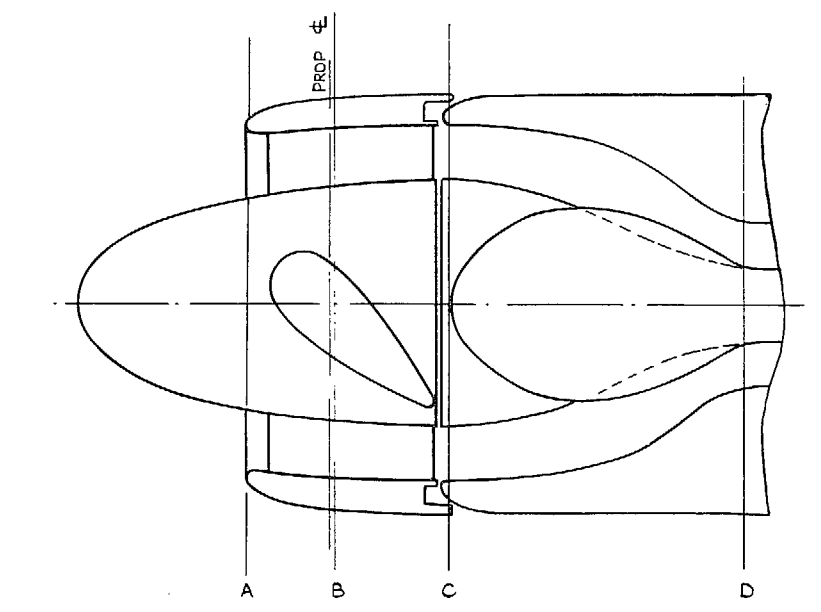

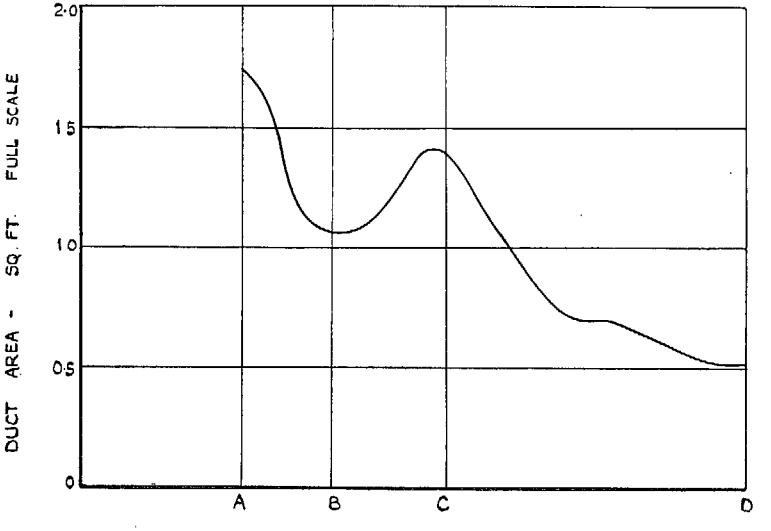

FIG. 5. Ducted spinner D/S/F.

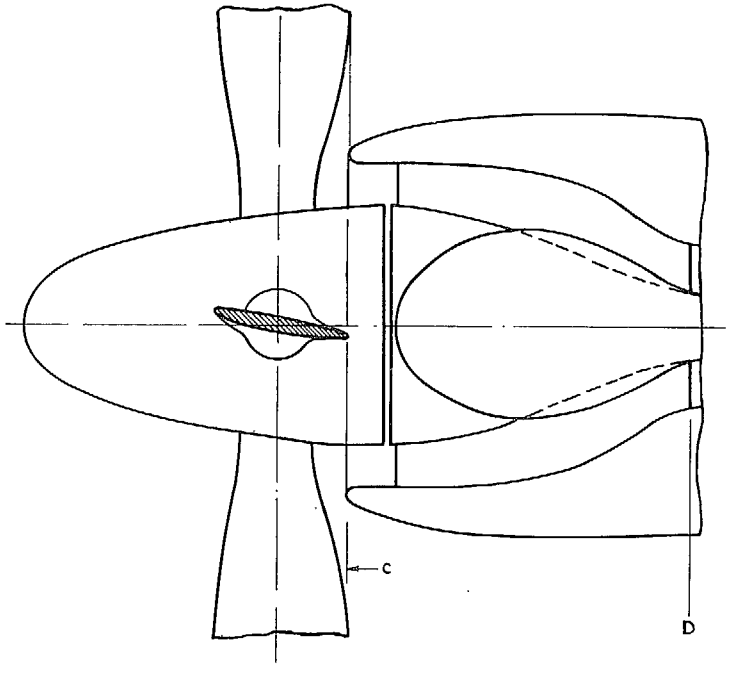

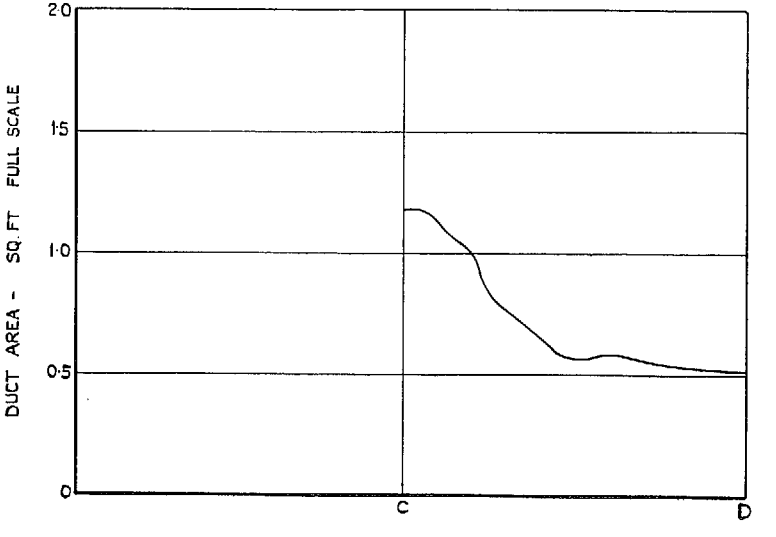

FIG. 6. Annular entry.

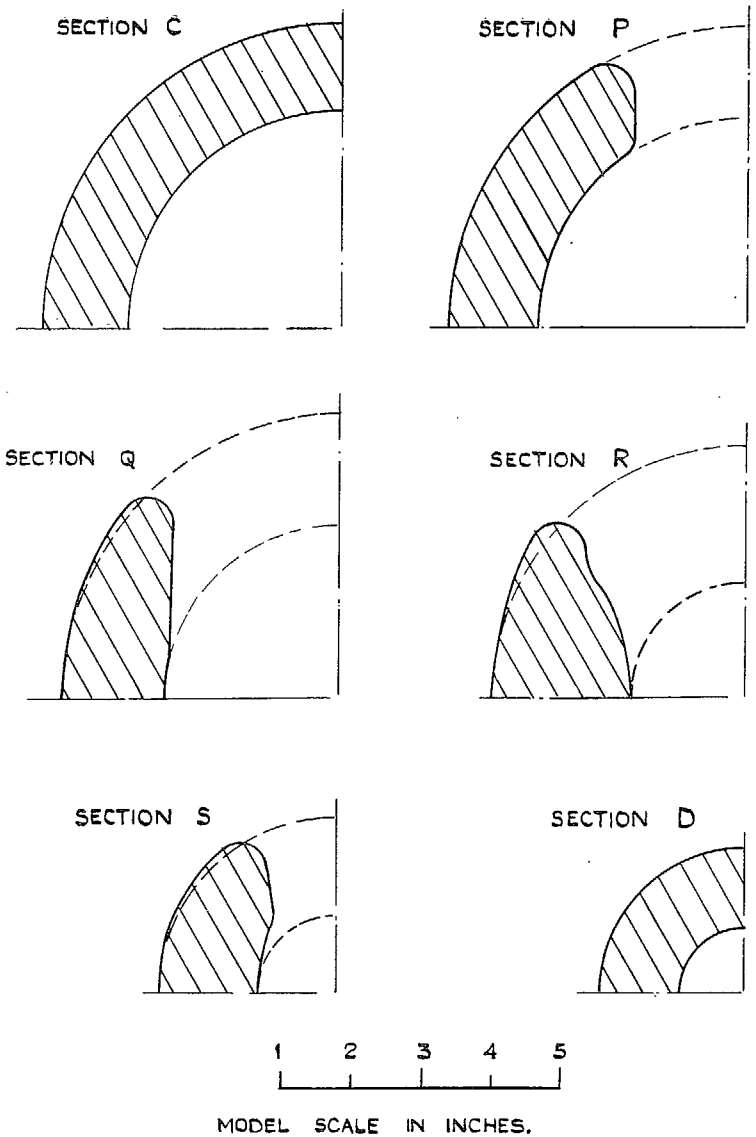

FULL LINES :- WITH REAR STRUTS (ENTRIES D/L/F D/L/C & D/S/F)
DOTTED LINES :- WITHOUT REAR STRUTS (ENTRY D/L/F/I)
POSITION OF SECTIONS IS SHOWN IN FIG. 4.

FIG. 7. Sections of rear duct with and without struts.

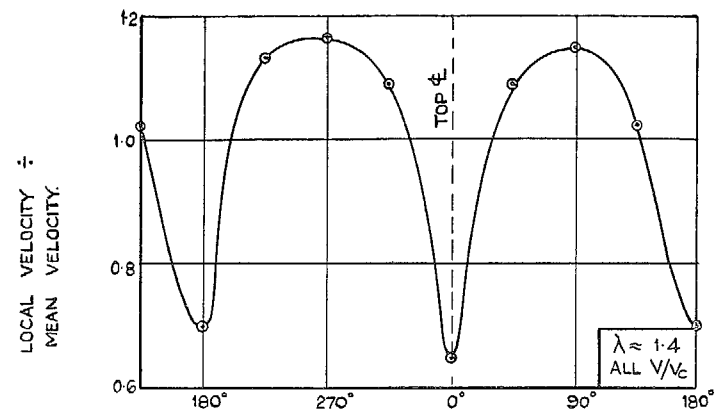

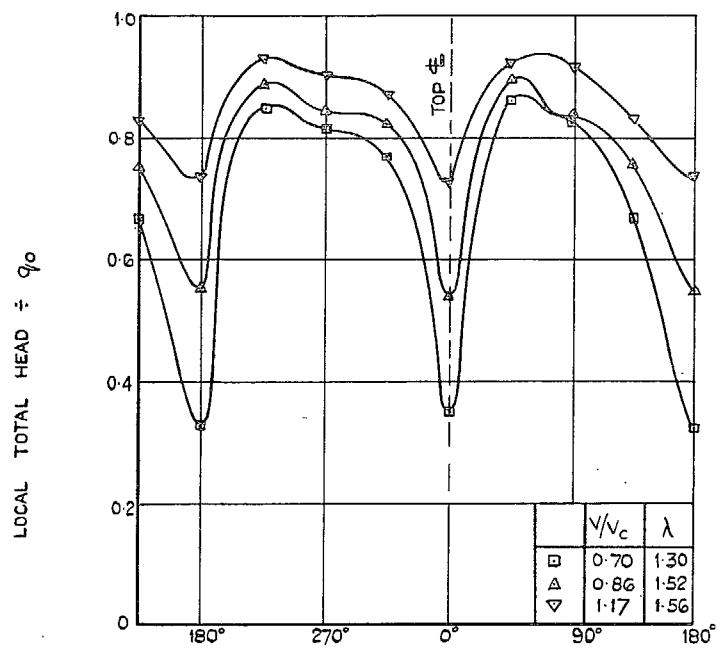

FIG. 8. Effect of rear struts on distribution at compressor inlet. Spinner D/S/F.

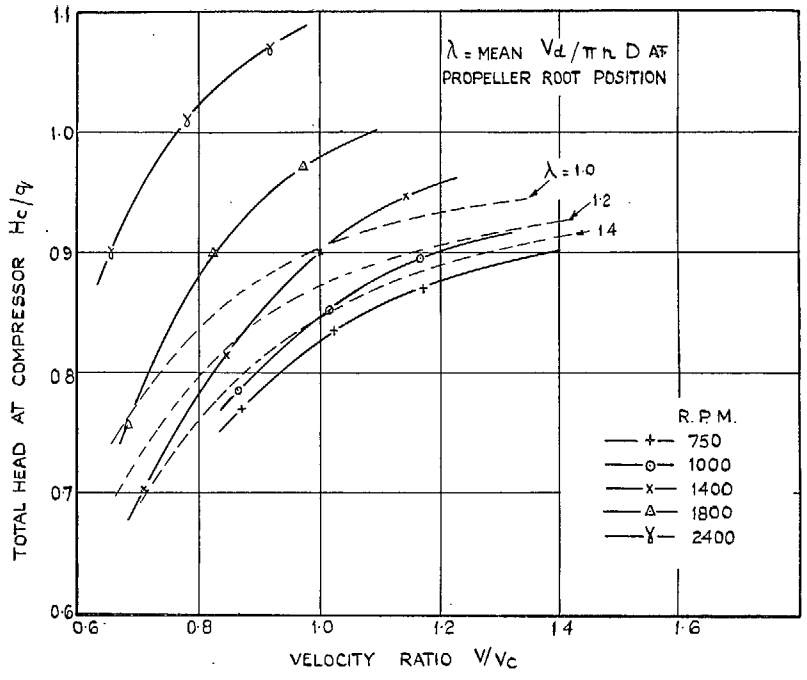

FIG. 9. Total head with spinner D/L/F.

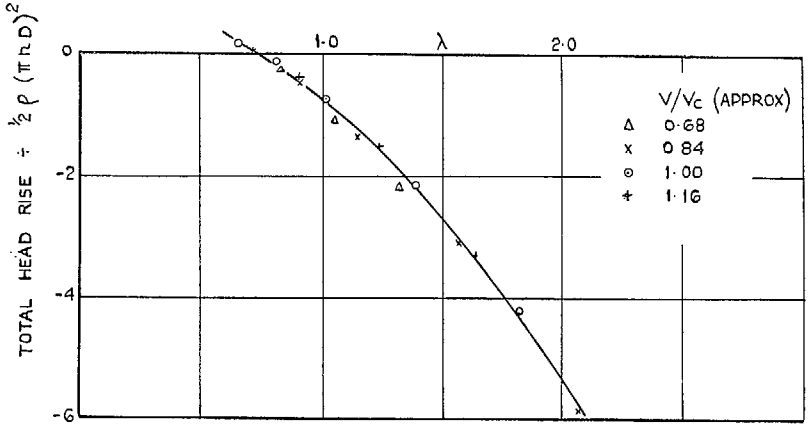

FIG. 10. Fan characteristic for spinner D/L/F.

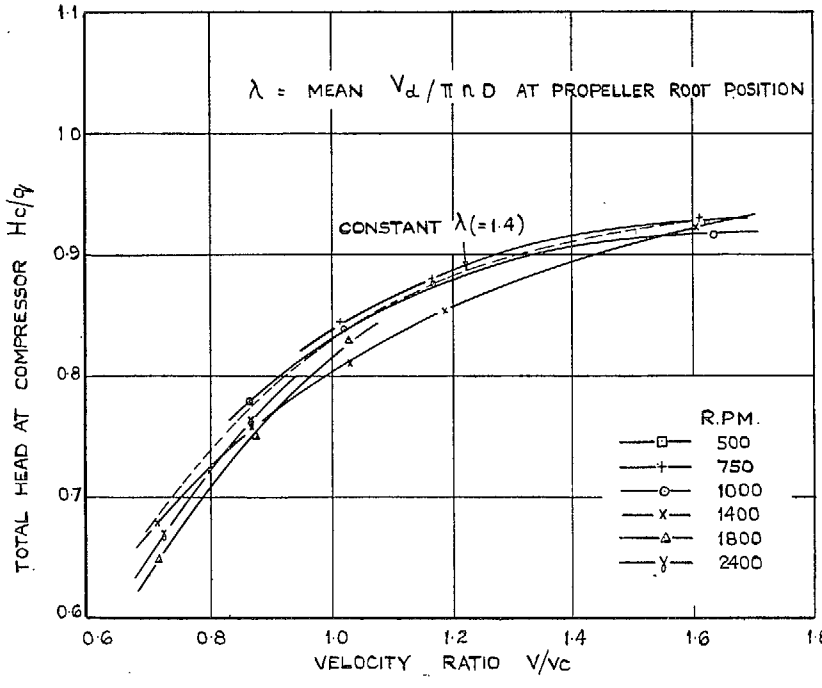

FIG. 11. Total head with spinner D/L/C.

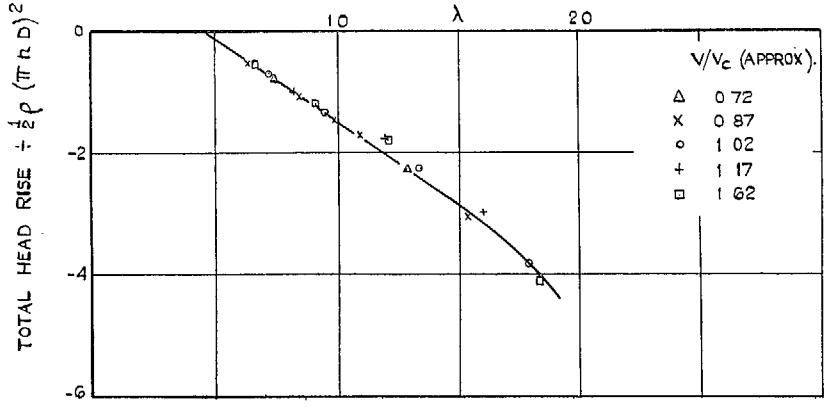

FIG. 12. Fan characteristic for spinner D/L/C.

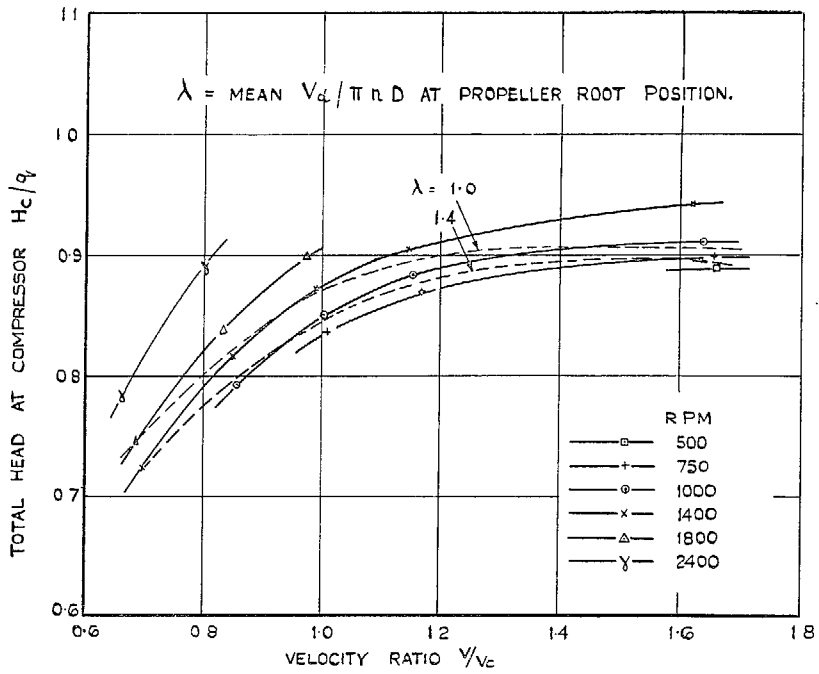

FIG. 13. Total head with spinner D/S/F.

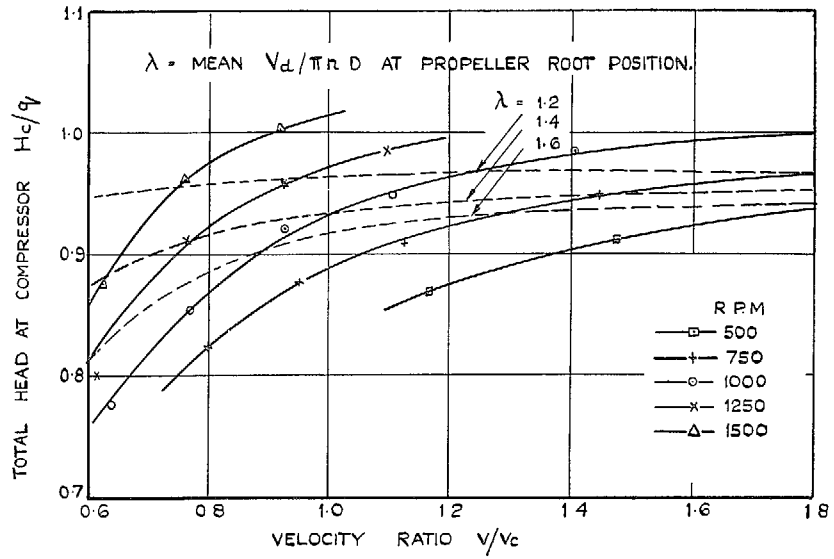

FIG. 15. Total head with spinner D/L/F/I.

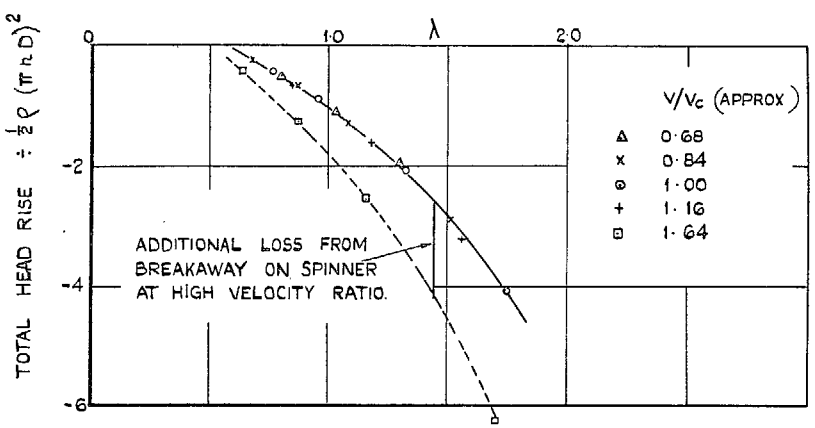

FIG. 14. Fan characteristic for spinner D/S/F.

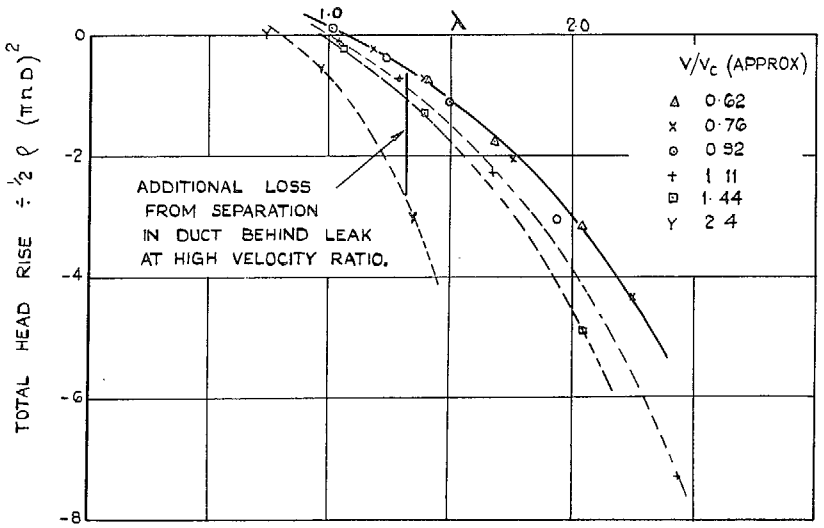

FIG. 16. Fan characteristic for spinner D/L/F/I.

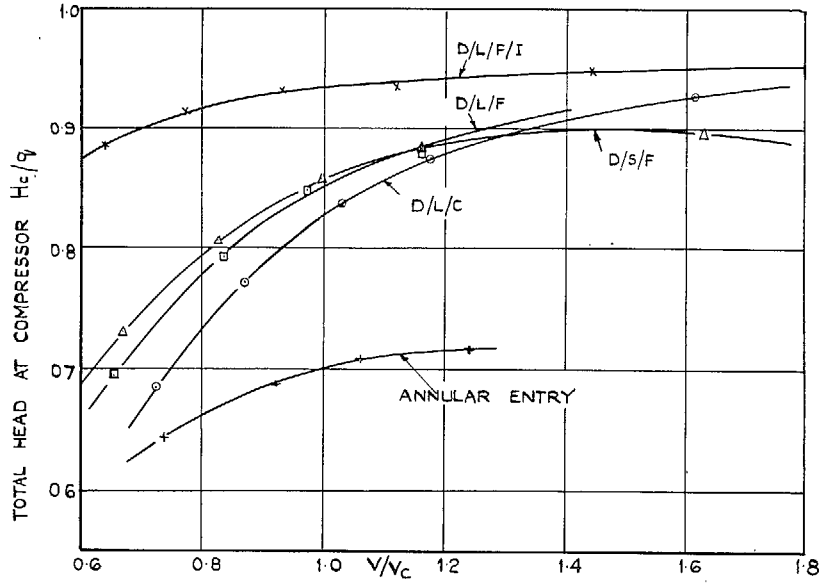

FIG. 17. Total head of various entries at $\lambda=1\cdot4$.

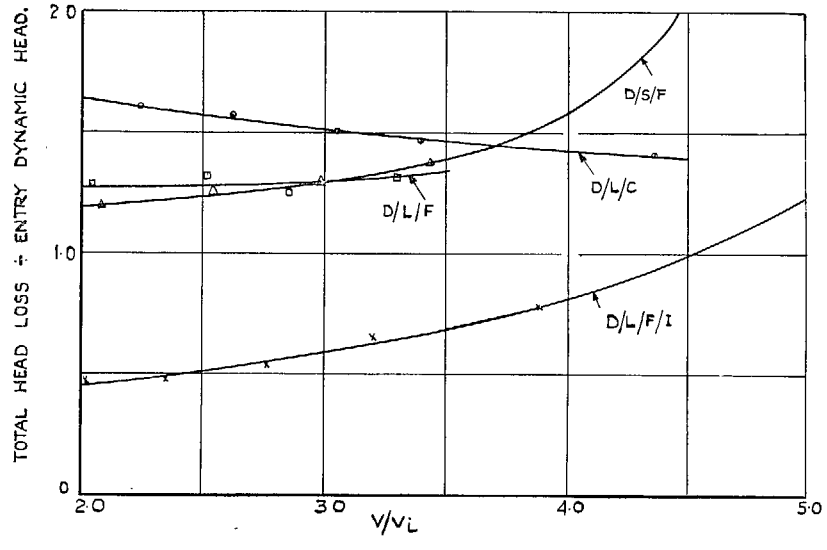

FIG. 18. Loss coefficient of various entries at $\lambda=1\cdot4$.

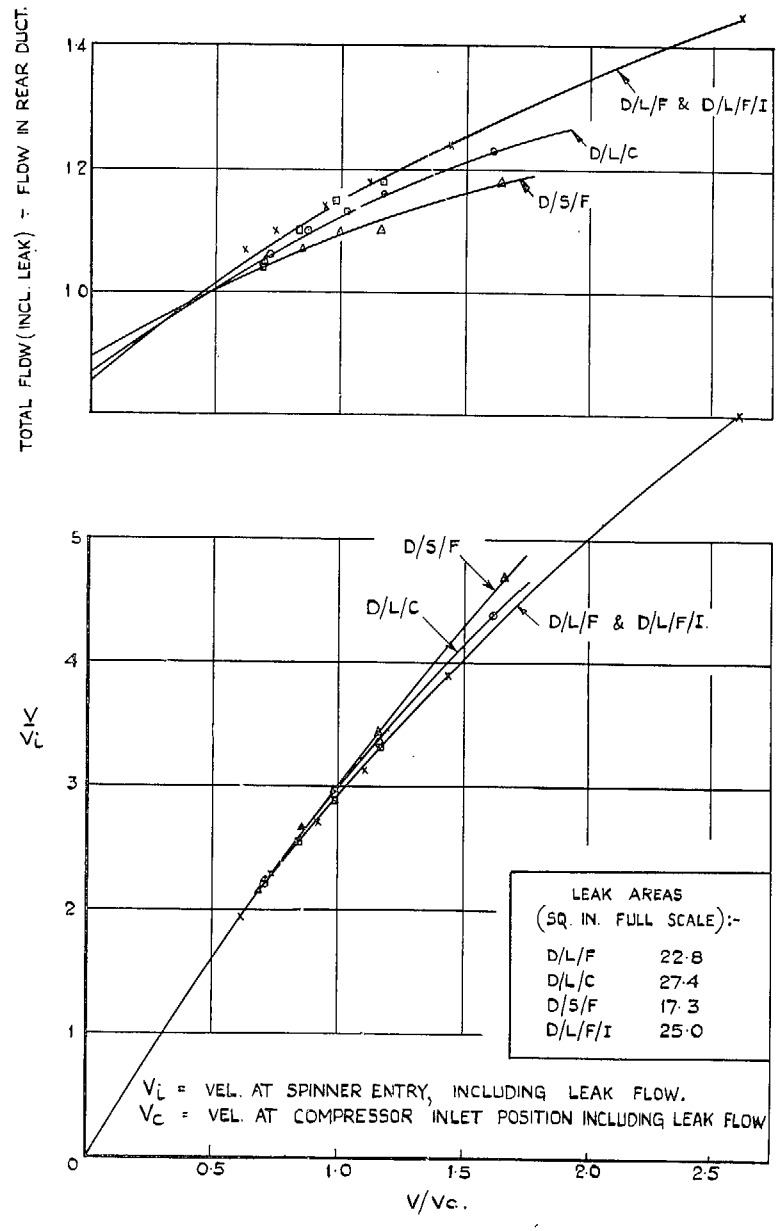

FIG. 19. Leak flow and relation between velocity ratios.

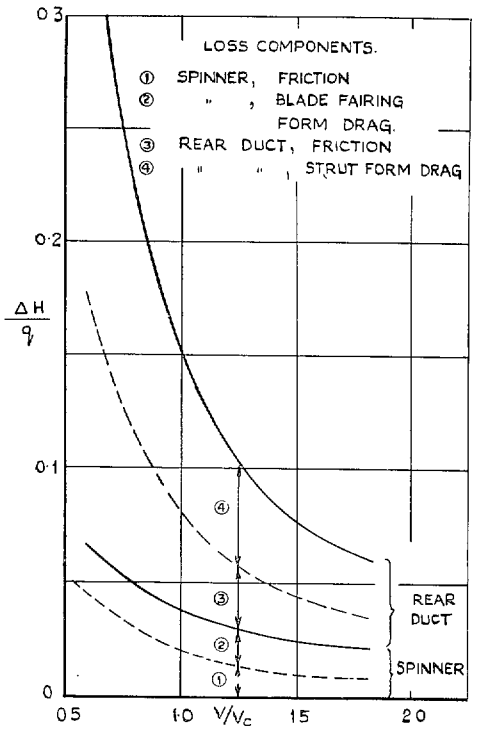

FIG. 20. Spinner D/L/F.

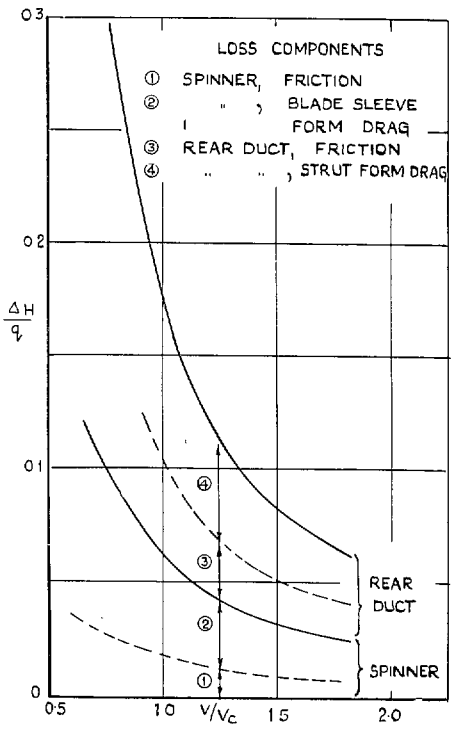

FIG. 21. Spinner D/L/C.

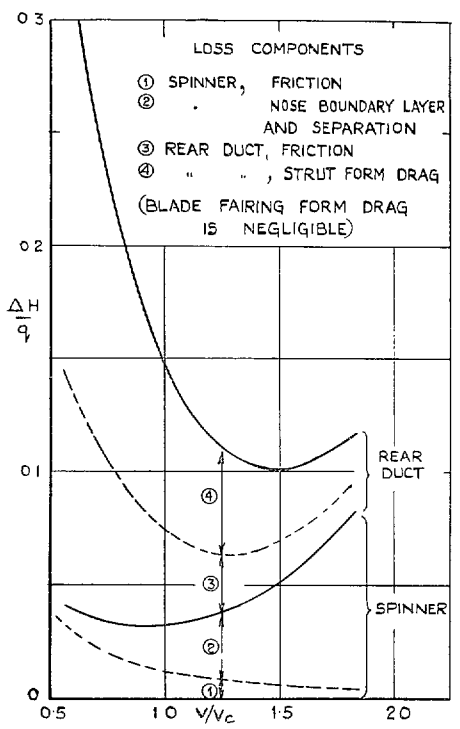

FIG. 22. Spinner D/S/F.

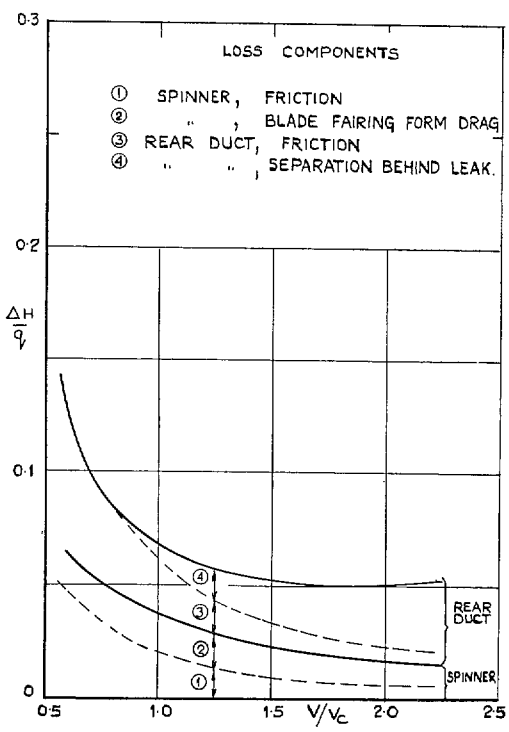

FIG. 23. Spinner D/L/F/I.

J4306 Wt.17/680 K9 9/54 D&Co. 34/263

PRINTED IN GREAT BRITAIN

Publications of the Aeronautical Research Council

ANNUAL TECHNICAL REPORTS OF THE AERONAUTICAL RESEARCH COUNCIL (BOUND VOLUMES)

1936 Vol. I. Aerodynamics General, Performance, Airscrews, Flutter and Spinning. 40*s.* (41*s.* 1*d.*).

Vol. II. Stability and Control, Structures, Seaplanes, Engines, etc. 50*s.* (51*s.* 1*d.*)

1937 Vol. I. Aerodynamics General, Performance, Airscrews, Flutter and Spinning. 40*s.* (41*s.* 1*d.*)

Vol. II. Stability and Control, Structures, Seaplanes, Engines, etc. 60*s.* (61*s.* 1*d.*)

1938 Vol. I. Aerodynamics General, Performance, Airscrews. 50*s.* (51*s.* 1*d.*)

Vol. II. Stability and Control, Flutter, Structures, Seaplanes, Wind Tunnels, Materials. 30*s.* (31*s.* 1*d.*)

1939 Vol. I. Aerodynamics General, Performance, Airscrews, Engines. 50*s.* (51*s.* 1*d.*)

Vol. II. Stability and Control, Flutter and Vibration, Instruments, Structures, Seaplanes, etc. 63*s.* (64*s.* 2*d.*)

1940 Aero and Hydrodynamics, Aerofoils, Airscrews, Engines, Flutter, Icing, Stability and Control, Structures, and a miscellaneous section. 50*s.* (51*s.* 1*d.*)

1941 Aero and Hydrodynamics, Aerofoils, Airscrews, Engines, Flutter, Stability and Control, Structures. 63*s.* (64*s.* 2*d.*)

1942 Vol. I. Aero and Hydrodynamics, Aerofoils, Airscrews, Engines. 75*s.* (76*s.* 3*d.*)

Vol. II. Noise, Parachutes, Stability and Control, Structures, Vibration, Wind Tunnels. 47*s.* 6*d.* (48*s.* 7*d.*)

1943 Vol. I. Aerodynamics, Aerofoils, Airscrews, 80*s.* (81*s.* 4*d.*)

Vol. II. Engines, Flutter, Materials, Parachutes, Performance, Stability and Control, Structures. 90*s.* (91*s.* 6*d.*)

1944 Vol. I. Aero and Hydrodynamics, Aerofoils, Aircraft, Airscrews, Controls. 84*s.* (85*s.* 8*d.*)

Vol. II. Flutter and Vibration, Materials, Miscellaneous, Navigation, Parachutes, Performance, Plates, and Panels, Stability, Structures, Test Equipment, Wind Tunnels. 84*s.* (85*s.* 8*d.*)

ANNUAL REPORTS OF THE AERONAUTICAL RESEARCH COUNCIL—

1933–34	1*s.* 6*d.* (1*s.* 8*d.*)	1937	2*s.* (2*s.* 2*d.*)
1934–35	1*s.* 6*d.* (1*s.* 8*d.*)	1938	1*s.* 6*d.* (1*s.* 8*d.*)
April 1, 1935 to Dec. 31, 1936.	4*s.* (4*s.* 4*d.*)	1939–48	3*s.* (3*s.* 2*d.*)

INDEX TO ALL REPORTS AND MEMORANDA PUBLISHED IN THE ANNUAL TECHNICAL REPORTS, AND SEPARATELY—

April, 1950 – – – – R. & M. No. 2600. 2*s.* 6*d.* (2*s.* 7½*d.*)

AUTHOR INDEX TO ALL REPORTS AND MEMORANDA OF THE AERONAUTICAL RESEARCH COUNCIL—

1909–1949 – – – – – R. & M. No. 2570. 15*s.* (15*s.* 3*d.*)

INDEXES TO THE TECHNICAL REPORTS OF THE AERONAUTICAL RESEARCH COUNCIL—

December 1, 1936 — June 30, 1939.	R. & M. No. 1850.	1*s.* 3*d.* (1*s.* 4½*d.*)
July 1, 1939 — June 30, 1945.	R. & M. No. 1950.	1*s.* (1*s.* 1½*d.*)
July 1, 1945 — June 30, 1946.	R. & M. No. 2050.	1*s.* (1*s.* 1½*d.*)
July 1, 1946 — December 31, 1946.	R. & M. No. 2150.	1*s.* 3*d.* (1*s.* 4½*d.*)
January 1, 1947 — June 30, 1947.	R. & M. No. 2250.	1*s.* 3*d.* (1*s.* 4½*d.*)
July, 1951 – – – –	R. & M. No. 2350.	1*s.* 9*d.* (1*s.* 10½*d.*)

Prices in brackets include postage.

Obtainable from

HER MAJESTY'S STATIONERY OFFICE

York House, Kingsway, London W.C.2 ; 423 Oxford Street, London W.1 (Post Orders : P.O. Box No. 569, London S.E.1) ; 13A Castle Street, Edinburgh 2 ; 39 King Street, Manchester 2 ; 2 Edmund Street, Birmingham 3 ; 1 St. Andrew's Crescent, Cardiff ; Tower Lane, Bristol 1 ; 80 Chichester Street, Belfast OR THROUGH ANY BOOKSELLER

S.O. Code No. 23-2894